HHS Public Access

Author manuscript

Cell. Author manuscript; available in PMC 2019 May 03.

Published in final edited form as:

Cell. 2018 May 03; 173(4): 920–933.e13. doi:10.1016/j.cell.2018.02.055.

IRF8 regulates transcription of *Naip*s for NLRC4 inflammasome activation

Rajendra Karki[1,#], **Ein Lee**[1,2,#], **David Place**[1], **Parimal Samir**[1], **Jayadev Mavuluri**[1], **Bhesh Raj Sharma**[1], **Arjun Balakrishnan**[1], **R. K. Subbarao Malireddi**[1], **Rechel Geiger**[1], **Qifan Zhu**[1,2], **Geoffrey Neale**[3], and **Thirumala-Devi Kanneganti**[1,4]

[1]Department of Immunology, St. Jude Children's Research Hospital, Memphis, TN, 38105, USA

[2]Integrated Biomedical Sciences Program, University of Tennessee Health Science Center, Memphis, TN, 38163, USA

[3]Hartwell Center for Bioinformatics & Biotechnology, St. Jude Children's Research Hospital, Memphis, TN, 38105, USA

SUMMARY

Inflammasome activation is critical for host defense against various microbial infections. Activation of the NLRC4 inflammasome requires detection of flagellin or type III secretion system (T3SS) components by NLR family apoptosis inhibitory proteins (NAIPs); yet how this pathway is regulated is unknown. Here we found that interferon regulatory factor 8 (IRF8) is required for optimal activation of the NLRC4 inflammasome in bone marrow-derived macrophages infected with *Salmonella* Typhimurium, *Burkholderia thailandensis,* or *Pseudomonas aeruginosa* but is dispensable for activation of the canonical and non-canonical NLRP3, AIM2, and Pyrin inflammasomes. IRF8 governs the transcription of *Naip*s to allow detection of flagellin or T3SS proteins to mediate NLRC4 inflammasome activation. Furthermore, we found that IRF8 confers protection against bacterial infection *in vivo*, owing to its role in inflammasome-dependent cytokine production and pyroptosis. Altogether, our findings suggest that IRF8 is a critical regulator of NAIPs and NLRC4 inflammasome activation for defense against bacterial infection.

Graphical Abstract

Correspondence: Thirumala-Devi.Kanneganti@StJude.org (T.-D.K).
[4]Lead Contact
[#]These authors contributed equally.

DECLARATION OF INTERESTS

The authors declare no competing financial interests.

AUTHOR CONTRIBUTIONS

R.K., E.L., and T.-D.K. conceptualized the study; R.K., E.L., D.P., P.S., J.M., A.B. and R.K.S.M. designed the methodology; R.K., E.L., D.P., P.S., J.M., B.R.S., A.B., R.K.S.M., R.G. and Q.Z. performed the experiments; R.K., E.L., D.P., P.S., J.M., B.R.S., A.B., R.K.S.M and G.N. conducted the analysis; R.K., E.L., and T.-D.K. wrote the manuscript with input from all authors. T.-D.K. acquired the funding and provided overall supervision.

Optimal activation of the NLRC4 activation in response to pathogenic bacteria is dependent on the factor IRF8.

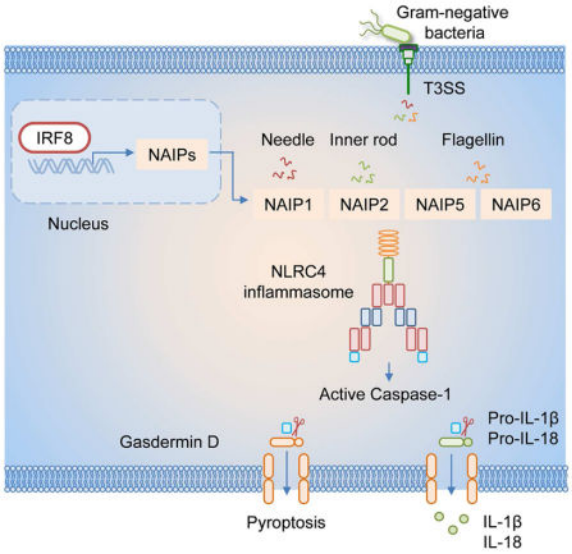

Keywords

NLRC4; inflammasome; IRF8; ICSBP; interferon regulatory factor; IRF; ALR; NLR; NAIP; caspase-1; PU.1; SPI1; *Burkholderia*; *Pseudomonas*; *Salmonella*; pathogen; type I interferon; infection; immunity; infectious diseases

INTRODUCTION

Type I interferons (IFNs) are secreted polypeptides that govern a vast array of functions ranging from anti-viral immunity to cancer immunosurveillance. During microbial infection, IFNs are rapidly induced to launch a potent host response primarily achieved by induction of IFN–stimulated genes that mediate pathogen clearance (Ivashkiv and Donlin, 2014; Zitvogel et al., 2015). Multiple intersections exist between type I IFN signaling and inflammasome activation. Inflammasomes are molecular platforms that assemble upon sensing various intracellular stimuli to process caspase-1 into its active form, allowing production of mature IL-1β and IL-18 (Man and Kanneganti, 2015). Caspase-1 activation via the caspase-11–dependent non-canonical NLR family, pyrin domain containing 3 (NLRP3) inflammasome requires type I IFNs (Rathinam et al., 2012). Bone marrow–derived macrophages (BMDMs) from IFN α/β receptor (IFNAR) knockout mice have impaired caspase-11 induction (Rathinam et al., 2012) and processing (Broz et al., 2012) in response to Gram-negative bacteria. Moreover, type I IFNs are required for the activation of the Absent in melanoma 2 (AIM2) inflammasome in response to the facultative intracellular bacteria *Francisella* (Fernandes-Alnemri et al., 2010; Henry et al., 2007), mediated by IFN regulatory factor 1 (IRF1) (Man et al., 2015). Yet the role of type I IFNs and IRFs in regulating other inflammasomes, including NLR family CARD domain containing 4 (NLRC4) and Pyrin inflammasomes, requires further investigation.

IRFs are a family of transcription factors that were first identified to regulate type I IFNs and type I IFN–induced genes (Tamura et al., 2008). Pioneering studies addressed IRF1 as a regulator for type I IFN production, however, IFN-α and IFN-β levels were normal in IRF1-deficient mouse embryonic fibroblasts following viral infection (Fujita et al., 1989; Matsuyama et al., 1993). IRF3 and IRF7 are now recognized as the major transcription factors for virus-induced type I IFN production (Sato et al., 2000). IRF9 is a component of the transcriptional activator IFN-stimulated gene factor 3 (ISGF3) required for type I IFN signaling (Veals et al., 1992). IRF8, also known as IFN consensus sequence binding protein (ICSBP), participates in IFN induction in a context-dependent manner (Tailor et al., 2007). IRF1 and IRF8 are both basally present in macrophages and inducible by IFNs and LPS (Barber et al., 1995; Driggers et al., 1990; Harada et al., 1989; Lehtonen et al., 1997). They cooperatively promote transcription of genes important for macrophage function such as IL-12 and iNOS (Liu et al., 2004; Masumi et al., 2002; Wang et al., 2000; Xiong et al., 2003). Based on the interaction of these two IRFs (Bovolenta et al., 1994), their importance in cellular immunity, and the requirement of IRF1 for AIM2 inflammasome activation in *F. novicida* infection, we investigated whether IRF8 has a similar role in inflammasome activation.

The NLRC4 inflammasome relies on NLR family apoptosis inhibitory proteins (NAIPs) for sensing bacterial components in the cytosol (Zhao and Shao, 2015). C57BL/6 mice have multiple *Naip* genes which encode cytosolic receptors for NLRC4 inflammasome assembly (Zhao and Shao, 2015). Yeast two-hybrid and mouse genetic studies have established a ligand-specific role of NAIP proteins in NLRC4 inflammasome activation. NAIP1 and NAIP2 detect needle and rod proteins of the bacterial type 3 secretion system (T3SS), respectively, whereas NAIP5 and NAIP6 recognize flagellin (Kofoed and Vance, 2011; Rauch et al., 2016; Zhao et al., 2011, 2016). On the other hand, humans have a single NAIP that senses needle and flagellin (Kortmann et al., 2015; Yang et al., 2013). Although the specific ligands for NLRC4 inflammasome have been examined in detail, upstream regulators have remained unexplored.

Here, we discovered a novel role of IRF8 in optimal activation of the NLRC4 inflammasome. Our findings show that IRF8 is a transcriptional regulator of *Naip*s that are prerequisite for NLRC4 inflammasome activation, ultimately contributing to host defense against bacterial pathogens.

RESULTS

IRF8 is dispensable for AIM2, NLRP3, and Pyrin inflammasome activation

The agent responsible for causing tularemia in humans, *Francisella tularensis,* uses multiple strategies to evade immune surveillance (Jones et al., 2012). Importantly, AIM2 detects the double-stranded DNA of the bacterium following its exposure in cytosol (Fernandes-Alnemri et al., 2010; Jones et al., 2010a). *F. tularensis* subspecies *novicida* (*F. novicida*) induced AIM2 inflammasome–dependent cleavage of pro-caspase-1 (p45) into active caspase-1 (p20) and subsequently produced mature cytokines IL-1β and IL-18, ultimately leading to cell death in unprimed wild-type (WT) BMDMs. *Irf8*$^{-/-}$ BMDMs were equally capable of cleaving caspase-1 as WT, producing IL-1β and IL-18, and pyroptosis following

F. novicida infection, suggesting IRF8 had no role in AIM2 inflammasome activation (Figures 1A–1C and S1A). Because IRF8 is involved in the development of immune cells (Kurotaki and Tamura, 2016), we examined the macrophage markers F4/80 and CD11b. The enrichment of double-positive cell populations in *Irf8*$^{-/-}$ BMDMs was comparable to that in WT BMDMs, indicative of normal *in vitro* macrophage differentiation (Figure S2A). Our group previously demonstrated that IRF1 is required to induce GBP2 and GBP5, which mediate killing of *F. novicida* and liberation of bacterial DNA to induce AIM2 inflammasome activation (Man et al., 2015). In *Irf8*$^{-/-}$ BMDMs, the protein levels of GBP2 and GBP5 were similar to those of control (Figure S2B). IRF1 is dispensable for cytosolic poly(dA:dT)-mediated AIM2 inflammasome activation (Man et al., 2015). To investigate the requirement of IRF8 in response to poly(dA:dT), we transfected poly(dA:dT) into WT and *Irf8*$^{-/-}$ BMDMs. Caspase-1 activation, IL-18 levels, and cell death in poly(dA:dT)-transfected BMDMs from WT or *Irf8*$^{-/-}$ mice were comparable (Figures 1D–1F and S1B). Similarly, we did not observe a significant difference in canonical NLRP3 inflammasome (Figures 1G–1I and S1C) or non-canonical NLRP3 inflammasome activation (Figures 1J–1L and S1D). The levels of inflammasome-independent cytokines (IL-6, TNF, and KC) were largely unaffected by the absence of IRF8 (Figure S1).

Pyrin inflammasome activation is triggered by the inactivation of Rho GTPases, which can be caused by bacterial cytotoxins (Xu et al., 2014). Toxin from *C. difficile* AB+ strain induced Pyrin inflammasome activation that was not mediated by IRF8 (Figures 1M–1O). These results excluded the requirement of IRF8 for AIM2, NLRP3, and Pyrin inflammasome activation.

IRF8 is required for optimal NLRC4 inflammasome activation

The NLRC4 inflammasome is critical for determining the response to bacterial pathogens that have gained access to the cytosol. *Salmonella*, a Gram-negative bacteria whose primary route of infection in mice and humans is through the gastrointestinal tract, was one of the first microbes identified to activate the NLRC4 inflammasome (Mariathasan et al., 2004). Other bacterial species characterized to engage NLRC4 inflammasome are *Pseudomonas aeruginosa*, *Burkholderia thailandensis*, and *Legionella pneumophila* (Amer et al., 2006; Sutterwala et al., 2007; Zamboni et al., 2006; Zhao et al., 2011). We infected WT BMDMs with *Salmonella enterica* subspecies *enterica* serovar Typhimurium (*S.* Typhimurium), which resulted in robust caspase-1 activation (Figure 2A). Surprisingly, reduced caspase-1 activation was observed in infected *Irf8*$^{-/-}$ BMDMs (Figure 2A and S2C). IL-18 and IL-1β production was dampened, with fewer pyroptotic cells (Figures 2B, 2C and S3A). Collectively, all features of caspase-1 activation were attenuated in the absence of IRF8 in response to *S.* Typhimurium infection.

Many pathogenic bacteria including *Salmonella* species harbor flagella and the evolutionarily related T3SS as important virulence mechanisms, which activate the NLRC4 inflammasome. Flagellin monomers form the filamentous flagellum that confers motility. The T3SS is composed of a basal body, connecting rod, and needle that altogether serves as a molecular syringe to inject various effector proteins into the host cytosol, inflicting intracellular perturbations beneficial to the invasion of the bacterium (Crowley et al., 2016;

Fàbrega and Vila, 2013; Storek and Monack, 2015). Previous studies have utilized flagellin-mutant *S.* Typhimurium to delineate the specific role of flagellin in activating the NLRC4 inflammasome (Franchi et al., 2006; Miao et al., 2006). *S.* Typhimurium lacking flagellin proteins FliC and FljB (Δ*fliC*Δ*fljB*) was still able to elicit caspase-1 activation and cell death in WT BMDMs that was largely dependent on NLRC4 (Figures 2D, S3B, and S3C). Δ*fliC*Δ*fljB* can activate the NLRC4 inflammasome alternatively by T3SS (Zhao et al., 2011). Infection with Δ*fliC*Δ*fljB* in *Irf8*$^{-/-}$ BMDMs revealed reduced caspase-1 activation and cell death, suggesting that IRF8 is necessary for T3SS-dependent NLRC4 inflammasome activation (Figures 2D, S3B, and S3C). The residual caspase-1 cleavage observed in cells lacking NLRC4 might be due to NLRP3 inflammasome activation (Broz et al., 2010; Man et al., 2014). To address this question, we infected *Nlrp3*$^{-/-}$*Nlrc4*$^{-/-}$ BMDMs with Δ*fliC*Δ*fljB*, which exhibited defective caspase-1 activation, IL-18 production, and cell death (Figures 2E, 2F, S3B, and S3C). There are two versions of *Salmonella* T3SS that are encoded separately by *Salmonella* pathogenicity island-1 (SPI-1) and SPI-2. SPI-1 T3SS is expressed to promote cell invasion in early stages of infection until *Salmonella* establishes its replicative niche in the phagocytic compartment *Salmonella*-containing vesicle (SCV), where it downregulates flagellin and SPI-1 T3SS expression and switches to SP1-2 T3SS (Crowley et al., 2016). SPI-1 was critical for inflammasome activation in response to *S.* Typhimurium because the *ΔSPI-1* strain was unable to activate caspase-1 (Figure 2G). In contrast, *ΔSPI-2* infection was able to induce NLRC4 inflammasome–mediated caspase-1 activation, IL-18 secretion, and pyroptosis in WT BMDMs, and to a lesser degree, in *Irf8*$^{-/-}$ BMDMs (Figures 2H, 2I, S3B, and S3C). These results suggest that IRF8 plays a role in NLRC4 inflammasome activation that is dependent on functional SPI-1 T3SS of *Salmonella*.

We further investigated the contribution of IRF8 to NLRC4 inflammasome activation by infecting BMDMs with other bacteria that engage the NLRC4 inflammasome. *P. aeruginosa* activated caspase-1 in WT BMDMs, leading to IL-18 and IL-1β secretion and pyroptotic cell death. Indeed, *Irf8*$^{-/-}$ BMDMs had less caspase-1 activation, IL-18 and IL-1β, and cell death than WT (Figures 2J–2L, S2D, and S3D). Consistently, the extent of NLRC4 inflammasome activity was reduced in *Irf8*$^{-/-}$ BMDMs after infection with *B. thailandensis* (Figures 2M–2O, S2E, and S3E). However, there was no defect in inflammasome-independent cytokine production upon these bacterial infections (Figures S3A, S3D, and S3E). IRF8 is constitutively expressed and its expression does not change significantly under conditions that induce expression of a variety of pro-inflammatory cytokines. (Figures S2F). Further supporting our observations, silencing *Irf8* in BMDMs resulted in decreased caspase-1 cleavage compared to that of control siRNA-treated BMDMs infected with *S.* Typhimurium, but not in those infected with *F. novicida* (Figures S4A and S4B). In addition, caspase-1 activation in *Irf8*$^{-/-}$ BMDMs infected with *S.* Typhimurium was less than that of *Irf8*$^{+/-}$ BMDMs (Figures S4C and S4D). Altogether, our findings highlight the importance of IRF8 to enable recognition of bacterial components during infection for NLRC4 inflammasome activation.

IRF8 is required for expression of murine *Naip*s

NAIPs belong to the NLR family of pattern recognition receptors (PRRs) and contain repeats of the inhibitor of apoptosis (IAP) domain also known as the Baculovirus inhibitor of

apoptosis protein repeat (BIR) domain (Jones et al., 2016). Association of each NAIP with its specific bacterial protein drives assembly and activation of the NLRC4 inflammasome. In mice, the corresponding NAIPs and ligands are NAIP1 for the T3SS needle, NAIP2 for the T3SS inner rod, and NAIP5 and NAIP6 for flagellin (Zhao and Shao, 2015). Humans encode a single NAIP that has the highest sequence homology with murine NAIP1 and is able to recognize needle and flagellin (Kortmann et al., 2015; Yang et al., 2013). In our experiments with bacterial infection, we identified the requirement of IRF8 for optimal NLRC4 inflammasome activation (Figure 2). Following these observations, we performed microarray to examine possible differential regulation of innate immune sensors in WT and *Irf8*$^{-/-}$ BMDMs upon infection with *S.* Typhimurium. We found reduced expression of genes encoding for NAIP6, NAIP5, NAIP2, and NLRC4; all critical components of the NLRC4 inflammasome complex (Figure 3A).

To find the regulatory interactions involving the NLRC4 inflammasome, we first generated a network of interactions between IRF8 and NAIPs (not shown) where IRF8 physically interacted with IRF4. Interestingly, IRF4 has the greatest sequence homology with IRF8 and requires SPI1 (also known as PU.1) as a binding partner to govern transcriptional programs in the B-cell lineage (Yamagata et al., 1996). Our subsequent generation of an interaction network involving IRF4 and NAIPs revealed the co-expression between IRF8 and SPI1. Moreover, *Irf8* was co-expressed with *Naip2*, *Naip5*, *Naip6*, and *Nlrc4* but not with *Naip1*. The selected group of proteins exhibited clique-like properties, with each node being connected to most of the other nodes, suggesting a potential functional interaction (Figure 3B).

To address how NAIPs are being regulated by IRF8, we reanalyzed a published Chromatin immunoprecipitation-sequencing (ChIP-seq) dataset (Olsson et al., 2016). Sequences mapping to the promoter regions of *Naip2*, *Naip5* and *Naip6* were enriched, suggesting that their expression can be regulated by IRF8 transcription factor activity. We found no enrichment of sequences mapping to the *Naip1* promoter. Although we did not find enrichment in the promoter region of *Nlrc4*, we identified an IRF8 binding site in the intronic region. Transcription factor binding in the introns have previously been reported to regulate transcription of target genes (Martone et al., 2003; Tokuhiro et al., 2003; Wei et al., 2006). IRF8 binding in the intron might be regulating *Nlrc4* expression by increasing chromatin accessibility for other transcription factors (Figure 3C). Real-time PCR (RT-PCR) analysis confirmed that *Naip1*, *Naip2*, *Naip5*, and *Naip6* had reduced gene expression in response to *S.* Typhimurium or flagellin transfection in *Irf8*$^{-/-}$ BMDMs relative to WT BMDMs (Figures 3D and 3E). Importantly, there was a basal defect in the transcription of all the *Naip*s and *Nlrc4*, but not for the control gene *Nlrp3* (Figures 3D–3F). Collectively, we show that IRF8 likely has binding sites in *Naip* promoters, contributing to the steady-state expression of *Naip*s. IFN signaling is important for the regulation of IRF8 (Driggers et al., 1990). Therefore it might be possible that the molecules related to IFN production and signaling involve in the regulation of NAIPs. However we found similar gene expression of *Naip*s and *Nlrc4* in the BMDMs lacking IRF1, IRF3, IRF7, IRF3 and IRF7, IRF5, IRF9, IFNAR1, IFNAR2, STAT1, TRIF, MAVS, MDA5, cGAS, and STING, suggesting IRF8 specifically regulates *Naip*s independent of IFN signaling (Figure S5). Our interaction map reveals a close network between IRF8, IRF4, and Ets family member SPI1 (Figure 3B).

When we analyzed another published ChIP-seq dataset (Iwata et al., 2017), there was no enrichment of IRF4 binding to *Naip2* or *Naip5* promoters. (Figure 3G). In addition we checked for SPI1 binding sites (Langlais et al., 2016), where we found enrichment of SPI1 binding to *Naip1*, *Naip2*, *Naip5*, and *Naip6* loci. This data suggests that SPI1 might work in conjunction with IRF8 for the transcriptional regulation of *Naip*s (Figure 3H).

To validate IRF8 binding to *Naip* promoters found in the public ChIP analysis, we designed primer sets specific to the IRF8 consensus sequence at −590 and −390 on the promoter regions of *Naip2* and *Naip5*, respectively, to perform targeted ChIP-PCR. The samples immunoprecipitated with IRF8 antibody but not the control IgG antibody yielded amplified PCR products, suggesting the recruitment of IRF8 onto the *Naip2* and *Naip5* promoters (Figure 4A). Next, to gain further insight into the molecular mechanism of IRF8-mediated transcription of *Naip*s, we cloned the promoters of *Naip*2 or *Naip5* into a luciferase reporter vector. Luciferase expression was significantly upregulated in cells that were co-transfected with IRF8 compared to those transfected with empty vectors, which suggested that IRF8 regulates mRNA abundance of *Naip2* and *Naip5* at the level of transcription (Figure 4B). Furthermore we sought to confirm the direct recruitment of IRF8 to *Naip* promoters. To this end, we performed electrophoretic mobility shift assay (EMSA) where we observed IRF8 binding to *Naip2* and *Naip5* promoters in nuclear extracts from WT BMDMs (Figure 4C). To determine whether the binding was specific to IRF8, we utilized competitive EMSA and antibody-mediated super shift assays. Non-labeled *Naip2* or *Naip5* oligonucleotides successfully competed with the labeled probes and addition of IRF8 antibody abolished the migration of the IRF8-*Naip* promoter complex into the membrane (Figure 4C). Together, these results establish that IRF8 directly binds to the promoters of *Naip2* and *Naip5* to regulate their expression. To further corroborate these findings, we reconstituted IRF8 in $Irf8^{-/-}$ BMDMs. Compared to untreated or control-transfected cells, reconstitution of IRF8 increased the expression of *Naip1*, *Naip2*, *Naip5*, and *Naip6*. (Figure 4D). All these findings mechanistically prove that IRF8 regulates *Naip*s at the transcriptional level.

Furthermore we examined the role of IRF8 in the NLRC4 inflammasome response to bacterial flagellin and components of the T3SS apparatus. Flagellin treatment alone without the transfection agent DOTAP failed to induce processing of caspase-1. Intracellular delivery of flagellin led to caspase-1 activation in WT BMDMs but activation was greatly impaired in $Irf8^{-/-}$ BMDMs (Figures 5A and S4E). In line with these observations, inflammasome-dependent cytokines IL-18 and IL-1β were reduced whereas KC was unaffected by the absence of IRF8 (Figures 5B, S4F, and S4G). Correspondingly, BMDMs lacking IRF8 were compromised in their ability to undergo pyroptosis after flagellin transfection (Figures 5C and 5D). Because NAIP5 is the receptor for cytosolic flagellin recognition, we checked for inflammasome activation in $Naip5^{-/-}$ BMDMs transfected with flagellin. As expected, caspase-1 maturation and IL-18 production were diminished in cells lacking NAIP5 to a similar extent as seen in cells lacking NLRC4 (Figure S4H and S4I). $Irf8^{-/-}$ BMDMs also had decreased inflammasome activity in response to bacterial T3SS. Transfection of the needle protein PrgI or the rod protein PrgJ into $Irf8^{-/-}$ BMDMs resulted in reduced caspase-1 activation, IL-18 release, and cell death compared to that of WT (Figures 5E–J and S4J). These results demonstrate the significance of IRF8 for sterile NLRC4 inflammasome activation triggered by pure ligands of NAIPs.

Requirement of IRF8 in host defense against *S.* Typhimurium and *B. thailandensis*

NLRC4 inflammasome activation is required for bacterial clearance in *S.* Typhimurium infected mice (Carvalho et al., 2012). To examine the *in vivo* relevance of IRF8 we infected mice intraperitoneally with *S.* Typhimurium and monitored body weight change and mortality during the course of infection. Compared to WT mice, *Irf8*$^{-/-}$ mice exhibited rapid weight loss between day 1 and day 2 which was similar to the degree of wasting in *Nlrc4*$^{-/-}$ mice. On the other hand *Irf8*$^{+/-}$ mice followed the trend of WT mice, showing a gradual decrease in body weight and successive recovery (Figure 6A). All *Irf8*$^{-/-}$ mice succumbed to infection within 4 days, while during the same time 100% of the *Irf8*$^{+/-}$ and WT mice were still alive. We continued monitoring until day 12 in which the accumulated mortality of *Irf8*$^{+/-}$ and WT mice was about 50%. The high susceptibility of *Nlrc4*$^{-/-}$ mice, as reported (Carvalho et al., 2012), was comparable to that of *Irf8*$^{-/-}$ mice (Figure 6B). The accelerated mortality of mice lacking IRF8 or NLRC4 highlights the importance of early innate immune responses to contain the pathogen which in turn greatly affects the outcome of the infection. Moreover, *Irf8*$^{-/-}$ mice were more susceptible to *B. thailandensis* infection. Within 4 days all *Irf8*$^{-/-}$ mice died, but more than 50% of WT mice survived (Figure S6A). Interestingly, *Naip5*$^{-/-}$ mice were more susceptible to *S.* Typhimurium infection than WT mice but still more resistant than *Irf8*$^{-/-}$ or *Nlrc4*$^{-/-}$ mice (Figure 6B). This intermediate phenotype suggests that other NAIPs also contribute to mount NLRC4 inflammasome activation in response to *S.* Typhimurium infection *in vivo*.

The bacterial burden in the spleen and liver of *Irf8*$^{-/-}$ or *Nlrc4*$^{-/-}$ mice, but not *Naip5*$^{-/-}$ mice was greater than that of WT mice upon *S.* Typhimurium infection (Figures 6C and 6D). Similarly, *Irf8*$^{-/-}$ mice had increased bacterial burden in the lung, liver, and spleen after *B. thailandensis* infection compared to WT mice (Figure S6B). IL-18 levels in the spleen, liver, and serum of these mice were also assessed 3 days after *S.* Typhimurium infection, or 2 days after *B. thailandensis* infection. Less IL-18 was detected in the tissues and serum of *Irf8*$^{-/-}$ mice than in those of WT, reflecting defective inflammasome activation in response to infection in *Irf8*$^{-/-}$ mice (Figures 6E, 6F, and S6C). Furthermore we investigated the numbers of circulating blood cells from the peripheral blood of infected WT and *Irf8*$^{-/-}$ mice using an automated hematology analyzer. Relative to WT mice, *Irf8*$^{-/-}$ mice exhibited higher numbers of total white blood cells (WBCs), neutrophils, and lymphocytes 3 days after *S.* Typhimurium infection, whereas no significant differences were noted in the numbers of total monocytes, eosinophils, basophils, red blood cells (RBCs), or platelets (Figure S7A). Similarly, we found more circulating WBCs and neutrophils in *Irf8*$^{-/-}$ mice 2 days after *B. thailandensis* infection, suggesting that the susceptibility of IRF8-deficient mice to infection was not due to impaired immune cell production and circulation (Figure S7B). However, we observed more prominent recruitment of immune cells, which were largely composed of neutrophils, in the lungs of *B. thailandensis* infected WT mice than in the lungs of *Irf8*$^{-/-}$ mice (Figure S6D). This may be due to the decreased production of inflammasome dependent cytokines in IRF8-deficient mice.

The main effectors of inflammasome activation are the cytokines IL-1 and IL-18, and the recently identified pore-forming molecule gasdermin D (Kayagaki et al., 2015; Liu et al., 2016; Shi et al., 2015). We used the above *S.* Typhimurium infection model to further access

the relative contribution of cytokine production and pyroptosis in host defense. The body weight of *Il18*$^{-/-}$*Il1r*$^{-/-}$, *Gsdmd*$^{-/-}$, and *Casp1*$^{-/-}$ mice dropped significantly during the first few days of infection compared to WT mice (Figure 7A). In 4 days, all mice from the three knock-out genotypes succumbed to infection, without showing any significant difference between the groups (Figure 7B). In comparison to WT mice, the bacterial loads of *Gsdmd*$^{-/-}$ mice and *Il18*$^{-/-}$*Il1r*$^{-/-}$mice were greater, supporting the idea that inflammasome-dependent cytokines and cell death were both critical in mediating host defense against *S.* Typhimurium infection (Figure 7C).

Next, we examined *Naip* gene expression patterns in the spleen of WT and *Irf8*$^{-/-}$ mice before and after infection with *S.* Typhimurium. *Irf8*$^{-/-}$ mice had basally lower expression of *Naip1*, *Naip5*, *Naip6*, *Nlrc4*, but not *Naip2* than WT mice (Figures 6G–6K). In WT mice we observed significant reduction in the gene expression of *Naip1* and *Naip5* after infection, which might be due to reduction in the levels of *Irf8* (Figures 6G, 6I, and 6L). After infection, *Naip1* and *Naip6* gene expression remained lower in *Irf8*$^{-/-}$ mice compared to that of WT mice (Figures 6G and 6J). Similarly, we observed lower gene expression of *Naip1*, *Naip5*, and *Naip6* in the spleen of *Irf8*$^{-/-}$ mice compared to those of WT mice after *B. thailandensis* infection (Figures S6E and S6G). However, in the lungs we observed decreased expression of *Naip2* along with other *Naip*s and *Nlrc4* before and after *B. thailandensis* infection (Figures S6F and S6H). Thus, in the absence of IRF8, infected mice were not able to promote sufficient inflammasome activation due to the lack of *Naip*s expression. These data display an important role for IRF8 in regulating the NLRC4-dependent clearance of *S.* Typhimurium and *B. thailandensis*.

DISCUSSION

We identified the novel role of IRF8 as an upstream regulator of NAIPs, ultimately contributing to NLRC4 inflammasome activity. Transcription of NAIPs was dependent on IRF8, but there was no significant induction of *Naip*s *in vitro* and *in vivo* in response to infection. The residual expression of *Naip*s and NLRC4 inflammasome activity in the absence of IRF8 imply that other factors may also contribute to the transcription of NAIPs. IRF8 is known to be recruited with other transcription factors owing to its weak DNA-binding activity. IRF, AP-1, and Ets family transcription factors interact with IRF8 to bind to specific composite elements allowing combinatorial control over numerous genes (Bovolenta et al., 1994; Eklund et al., 1998; Glasmacher et al., 2012). In our network analysis IRF8 is co-expressed with IRF4 and SPI1. ChIP-Seq analysis indicated that SPI1 but not IRF4 binds to the promoter regions of *Naip*s. Therefore, it is also possible that SPI1 could function with IRF8 to regulate *Naip*s expression and NLRC4 inflammasome activation. Whether IRF8 and SPI1 share common binding sites for *Naip*s needs to be explored.

Due to the existence of compensatory mechanisms to combat infections, it is difficult to access the sole contribution of inflammasome activity. Nevertheless, the expulsion of bacteria-containing intestinal epithelial cells from *S.* Typhimurium-challenged mice well displays how the inflammasome promotes bacterial clearance. Mice lacking *Nlrc4* or *Naip*s have increased bacterial load locally and systemically (Sellin et al., 2014). Moreover IL-1

and IL-18, and gasdermin D mediated cell death directed by inflammasome activation were both important for host protection. Our *in vivo* data provide a striking example of how optimal NAIP/NLRC4 inflammasome activity, conferred by IRF8, is crucial for host survival. In addition to the regulation of inflammasome activation shown here, IRF8 also plays a critical role in development of cDC1s and pDCs (Sichien et al., 2016), which might also have contributed to the increased susceptibility of *Irf8*$^{-/-}$ mice to *Salmonella* and *Burkholderia* infections.

There was reduction of *Naip2* in the lungs but not the spleen of mice lacking IRF8, implying that additional regulatory or compensatory mechanisms may exist to modulate *Naip2* expression independently of IRF8 in certain cell types. Moreover the relative expression of *Naip*s varies among different cell types (Yang et al., 2013). In addition, bacteria produce different amounts of single or multiple NAIP ligands of varying affinity. Because of this combination of host factors and pathogen factors, the degree of NLRC4 inflammasome activation *in vivo* is complex (Zhao and Shao, 2015). Altogether, our work on IRF8 provides new insights into the regulation of the NAIP/NLRC4 inflammasome. The relationship among IRFs, the IFN signaling pathway, and inflammasomes remains to be further explored.

STAR★METHODS

KEY RESOURCES TABLE

The table highlights the genetically modified organisms and strains, cell lines, reagents, software, and source data **essential** to reproduce results presented in the manuscript. Depending on the nature of the study, this may include standard laboratory materials (i.e., food chow for metabolism studies), but the Table is **not** meant to be comprehensive list of all materials and resources used (e.g., essential chemicals such as SDS, sucrose, or standard culture media don't need to be listed in the Table). **Items in the Table must also be reported in the Method Details section within the context of their use.** The number of **primers and RNA sequences** that may be listed in the Table is restricted to no more than ten each. If there are more than ten primers or RNA sequences to report, please provide this information as a supplementary document and reference this file (e.g., See Table S1 for XX) in the Key Resources Table.

Please note that ALL references cited in the Key Resources Table ***must be included in the References list.*** Please report the information as follows:

- **REAGENT or RESOURCE:** Provide full descriptive name of the item so that it can be identified and linked with its description in the manuscript (e.g., provide version number for software, host source for antibody, strain name). In the Experimental Models section, please include all models used in the paper and describe each line/strain as: model organism: name used for strain/line in paper: genotype. (i.e., Mouse: OXTR$^{fl/fl}$: B6.129(SJL)-Oxtr$^{tm1.1Wsy/J}$). In the Biological Samples section, please list all samples obtained from commercial sources or biological repositories. Please note that software mentioned in the Methods Details or Data and Software Availability section needs to be also included in the

table. See the sample Table at the end of this document for examples of how to report reagents.

- **SOURCE:** Report the company, manufacturer, or individual that provided the item or where the item can obtained (e.g., stock center or repository). For materials distributed by Addgene, please cite the article describing the plasmid and include “Addgene” as part of the identifier. If an item is from another lab, please include the name of the principal investigator and a citation if it has been previously published. If the material is being reported for the first time in the current paper, please indicate as “this paper.” For software, please provide the company name if it is commercially available or cite the paper in which it has been initially described.
- **IDENTIFIER:** Include catalog numbers (entered in the column as “Cat#” followed by the number, e.g., Cat#3879S). Where available, please include unique entities such as RRIDs, Model Organism Database numbers, accession numbers, and PDB or CAS IDs. For antibodies, if applicable and available, please also include the lot number or clone identity. For software or data resources, please include the URL where the resource can be downloaded. Please ensure accuracy of the identifiers, as they are essential for generation of hyperlinks to external sources when available. Please see the Elsevier list of Data Repositories with automated bidirectional linking for details. When listing more than one identifier for the same item, use semicolons to separate them (e.g. Cat#3879S; RRID: AB_2255011). If an identifier is not available, please enter “N/A” in the column.
  - ***A NOTE ABOUT RRIDs:*** We highly recommend using RRIDs as the identifier (in particular for antibodies and organisms, but also for software tools and databases). For more details on how to obtain or generate an RRID for existing or newly generated resources, please visit the RII or search for RRIDs.

Please use the empty table that follows to organize the information in the sections defined by the subheading, skipping sections not relevant to your study. Please do not add subheadings. To add a row, place the cursor at the end of the row above where you would like to add the row, just outside the right border of the table. Then press the ENTER key to add the row. Please delete empty rows. Each entry must be on a separate row; do not list multiple items in a single table cell. Please see the sample table at the end of this document for examples of how reagents should be cited.

KEY RESOURCES TABLE

REAGENT or RESOURCE	SOURCE	IDENTIFIER
Antibodies		
Mouse monoclonal anti-caspase-1	Adipogen	Cat#AG-20B-0042; RRID: AB_2490248
Goat polyclonal anti-IRF8	Santa Cruz Biotechnology	Cat#sc-6058; RRID:AB_649510

REAGENT or RESOURCE	SOURCE	IDENTIFIER
Rabbit polyclonal anti-GBP2	Proteintech	Cat#11854-1-AP; RRID: AB_2109336
Rabbit polyclonal anti-GBP5	Proteintech	Cat#13220-1-AP; RRID: AB_2109348
Mouse monoclonal anti-β-actin	Proteintech	Cat#66009-1-Ig; RRID:AB_2687938
HRP–conjugated anti-rabbit	Jackson Immuno Research Laboratories	Cat#111-035-047; RRID:AB_2337940
HRP–conjugated anti-mouse	Jackson Immuno	Cat#315-035-047;
	Research Laboratories	RRID:AB_2340068
HRP–conjugated anti-goat	Jackson Immuno	Cat#705-035-003;
	Research Laboratories	RRID:AB_2340390
Rat monoclonal anti-CD11b	Affymetrix eBioscience	Cat#48-0112-82; RRID: AB_1582236
Rat monoclonal anti-F4/80	BioLegend	Cat#123109; RRID: AB_893498
Rabbit monoclonal anti-IRF8	Cell Signaling Technology	Cat#5628 RRID:AB_10828231
Normal rabbit IgG	Cell Signaling Technology	Cat#2729 RRID:AB_1031062
Bacterial and Virus Strains		
Francisella novicida strain U112	(Man et al., 2015)	N/A
Salmonella Typhimurium SL1344	(Man et al., 2015)	N/A
Salmonella Typhimurium SL1344 Δ*fliC*Δ*fljB*	(Man et al., 2015)	N/A
Salmonella Typhimurium SL1344 Δ*SPI-1*	(Man et al., 2015)	N/A
Salmonella Typhimurium SL1344 Δ*SPI-2*	(Broz et al., 2010)	N/A
Burkholderia thailandensis strain E264	Dr. Joseph Mougous (Schwarz et al., 2010)	N/A
Pseudomonas aeruginosa strain PAO1	Dr. Joseph Mougous (Hood et al., 2010)	N/A
Biological Samples		
Chemicals, Peptides, and Recombinant Proteins		
DMEM	ThermoFisher Scientific	Cat#11995-073
MEM Non-Essential Amino Acids Solution	ThermoFisher Scientific	Cat#11140-050
Fetal Bovine Serum	Biowest	Cat#S1620
Penicillin and Streptomycin	ThermoFisher Scientific	Cat#15070-063
BBL Trypticase Soy Broth	BD Biosciences	Cat#211768
L-cysteine	ThermoFisher Scientific	Cat#BP376-100
Luria-Bertani media	MP Biomedicals	Cat#3002-031
BBL Trypticase Soy Broth	BD Biosciences	Cat#211768
BBL brain heart infusion agar	BD Biosciences	Cat#211065
PBS	ThermoFisher Scientific	Cat#14190-250
Gentamicin	ThermoFisher Scientific	Cat#15750-060

REAGENT or RESOURCE	SOURCE	IDENTIFIER
Ultrapure LPS from *Salmonella minnesota* R595	InvivoGen	Cat#tlrl-smlps
ATP	Roche	Cat#10127531001
Poly(dA:dT)	InvivoGen	Cat#tlrl-patn
Opti-MEM	ThermoFisher Scientific	Cat#31985-070
Ultrapure flagellin from *S.* Typhimurium	InvivoGen	Cat#tlrl-epstfla-5
Recombinant *S.* Typhimurium PrgI	Mybiosource	Cat#MBS1177087
Recombinant *S.* Typhimurium PrgJ	Mybiosource	Cat#MBS2061410
DOTAP Liposomal Transfection Reagent	Roche	Cat#11202375001
Luminata Forte Western HRP Substrate	Millipore	Cat#WBLUF0500
TRIzol	ThermoFisher Scientific	Cat#15596026
SYBR Green	Applied Biosystems	Cat#4368706
GenMute siRNA Transfection Reagent	SignaGen Laboratories	Cat#SL100568
Protease inhibitor	Roche	Cat#11697498001
Phosphatase inhibitor	Roche	Cat#04906837001
FuGENE HD Transfection Reagent	Promega	Cat#E2311
Neon Transfection System Kit	ThermoFisher Scientific	Cat#MPK10025
Critical Commercial Assays		
Xfect transfection kit	Clontech Laboratories, Inc	Cat#631318
CytoTox 96 Non-Radioactive Cytotoxicity Assay	Promega	Cat#G1780
High capacity cDNA Reverse Transcription kit	Applied Biosystems	Cat#4368814
Ambion Wild-Type Expression kit	ThermoFisher Scientific	Cat# 4411973
Affymetrix GeneChip Mouse Gene 2.0 ST Array	ThermoFisher Scientific	Cat#902119
Multiplex ELISA kit	Millipore	Cat#MCYTOMAG-70K
IL-18 ELISA kit	Invitrogen	Cat#BMS618-3
Light Shift Chemiluminescent EMSA kit	ThermoFisher Scientific	Cat#20148
Dual-Luciferase Reporter Assay System	Promega	Cat#E1910
Deposited Data		
Microarray raw data	This paper	GEO: GSE110452
Experimental Models: Cell Lines		
HEK293T	ATCC#3216	Cat# CRL-3216; RRID:CVCL_0063
Experimental Models: Organisms/Strains		

REAGENT or RESOURCE	SOURCE	IDENTIFIER
Irf8$^{-/-}$ mice	Jackson Laboratory	RRID:IMSR_JAX:018298
Irf1$^{-/-}$ mice	(Matsuyama et al., 1993)	N/A
Nlrp3$^{-/-}$ mice	(Kanneganti et al., 2006)	N/A
Nlrc4$^{-/-}$ mice	(Franchi et al., 2006)	N/A
Nlrp3$^{-/-}$*Nlrc4*$^{-/-}$ mice	This paper (Mice crossed in our facility)	N/A
Aim2$^{-/-}$ mice	(Jones et al., 2010)	N/A
Pyrin$^{-/-}$ mice	(Gorp et al., 2016)	N/A
Naip5$^{-/-}$ mice	Dr. Russell Vance (Lightfield et al., 2008)	N/A
Il18$^{-/-}$*Il1r*$^{-/-}$ mice	(Glaccum et al., 1997; Takeda et al., 1998) (Mice crossed in our facility)	N/A
Gsdmd$^{-/-}$ mice	This paper (Generated in our facility)	N/A
Casp1$^{-/-}$ mice	(Man et al., 2017)	N/A
Casp11$^{-/-}$ mice	(Kayagaki et al., 2011)	N/A
Irf3$^{-/-}$ mice	(Sato et al., 2000)	N/A
Irf7$^{-/-}$ mice	(Honda et al., 2005)	N/A
Irf3$^{-/-}$ *Irf7*$^{-/-}$ mice	This paper (Mice crossed in our facility)	N/A
Irf9$^{-/-}$ mice	(Kimura et al., 1996)	N/A
Ifnar1$^{-/-}$ mice	(Müller et al., 1994)	N/A
Ifnar2$^{-/-}$ mice	(Fenner et al., 2006)	N/A
Stat1$^{-/-}$ mice	(Matsuyama et al., 1993)	N/A
Trif$^{-/-}$ mice	(Yamamoto et al., 2003)	N/A
Mavs1$^{-/-}$ mice	Dr. Michael Gale (Suthar et al., 2012)	N/A
Ifih1$^{-/-}$ (*Mda5*$^{-/-}$) mice	(Kato et al., 2006)	N/A
Mb21d1$^{-/-}$ (*Cgas*$^{-/-}$) mice	(Schoggins et al., 2014)	N/A
Tmem173$^{-/-}$ (*Sting*$^{gt/gt}$) mice	(Sauer et al., 2011)	N/A
Oligonucleotides		
siGENOME SMARTpool siRNA specific for the gene encoding mouse *Irf8*	Dharmacon	Cat#M-040737-00
RT-PCR *Naip1* Forward: 5′ - TGCCCAGTATATCCAAGGCTA-3′	This paper	N/A
RT-PCR *Naip1* Reverse: 5′ - AGACGCTGTCGTTGCAGTAAG-3′	This paper	N/A
RT-PCR *Naip2* Forward: 5′ - TTTTGTGAATCCCTGGGTCA-3′	This paper	N/A
RT-PCR *Naip2* Reverse: 5′ - TGTAGAAAAGGCCTGCTTTGA-3′	This paper	N/A
RT-PCR *Naip5* Forward: 5′ - AAGGAGATGACCCCTGGAAG-3′	This paper	N/A

REAGENT or RESOURCE	SOURCE	IDENTIFIER
RT-PCR *Naip5* Reverse: 5′-TGACCCAGGACTTCACAAAA-3′	This paper	N/A
RT-PCR *Naip6* Forward: 5′-TTTTGTGAAGTCCTGGGTCAG-3′	This paper	N/A
RT-PCR *Naip6* Reverse: 5′-CAATGTCCTTTTTGCCAGTG-3′	This paper	N/A
RT-PCR *Nlrc4* Forward: 5′-CAGGTGGTCTGATTGACAGC-3′	This paper	N/A
RT-PCR *Nlrc4* Reverse: 5′-CCCCAATGTCAGACAAATGA-3′	This paper	N/A
RT-PCR *Irf8* Forward: 5′-GATCGAACAGATCGACAGCA-3′	This paper	N/A
RT-PCR *Irf8* Reverse: 5′-GCTGGTTCAGCTTTGTCTCC-3′	This paper	N/A
RT-PCR *Nlrp3* Forward: 5′-TGCAGAAGACTGACGTCTCC-3′	This paper	N/A
RT-PCR *Nlrp3* Reverse: 5′-CGTACAGGCAGTAGAACAGTTC-3′	This paper	N/A
RT-PCR *Gapdh* Forward: 5′-CGTCCCGTAGACAAAATGGT-3′	This paper	N/A
RT-PCR *Gapdh* Reverse: 5′-TTGATGGCAACAATCTCCAC-3′	This paper	N/A
RT-PCR *Hprt* Forward: 5′-CTCATGGACTGATTATGGACAGGAC-3′	This paper	N/A
RT-PCR *Hprt* Reverse: 5′-GCAGGTCAGCAAAGAACTTATAGCC-3′	This paper	N/A
ChIP-PCR *Naip2* Forward: 5′-TTTCAACCTTACTACACTTTCAATCAAATAGAA-3′	This paper	N/A
ChIP-PCR *Naip2* Reverse: 5′-ATAGATAGATAGATATGGATATATAACC-3′	This paper	N/A
ChIP-PCR *Naip5* Forward: 5′-AGTGCTGACACATTTGATGCCACCAATGCA-3′	This paper	N/A
ChIP-PCR *Naip5* Reverse: 5′-GCCCCCTTGCTGCTGATGCTCTGTGACCAG-3′	This paper	N/A
Recombinant DNA		
pGL4.17[*luc2*/Neo] Vector	Promega	Cat#E6721
pRL-TK-Renilla	Promega	Cat#E2241
pCMV6-mIRF8	Origene	Cat#MR206748
pcDNA3.1	Invitrogen	Cat#V79020
Software and Algorithms		
GraphPad Prism 6.0	GraphPad Software, Inc.	http://www.graphpad.com
FlowJo software	FlowJo, LLC and Illumina, Inc	http://www.flowjo.com/
Partek Genomics Suite version 6.6	Partek	http://www.partek.com

REAGENT or RESOURCE	SOURCE	IDENTIFIER
Ingenuity Pathways Analysis software	Qiagen	https://www.qiagenbioinformatics.com/
Cytoscape	(Shannon et al., 2003)	http://www.cytoscape.org/
GeneMANIA Cytoscape plugin	(Mostafavi et al., 2008)	http://genemania.org/plugin
Gene Expression Omnibus (GEO)	(Edgar et al., 2002)	https://www.ncbi.nlm.nih.gov/geo/
MACS2	(Zhang et al., 2008)	
Tuxedo	(Trapnell et al., 2012)	
Integrative Genomics Viewer (IGV)	(Robinson et al., 2011)	http://software.broadinstitute.org/software/igv/
DAVID bioinformatics database 50	(Huang et al., 2009)	https://david.ncifcrf.gov/home.jsp
Other		
PVDF Membrane	Millipore	Cat#IPVH00010
Biodyne Nylon Membrane	ThermoFisher Scientific	Cat#77016

CONTACT FOR REAGENT AND RESOURCE SHARING

Further information and requests for reagents may be directed to, and will be fulfilled by the lead contact Thirumala-Devi Kanneganti (thirumala-devi.kanneganti@stjude.org).

EXPERIMENTAL MODELS AND SUBJECT DETAILS

Mice—*Irf8*$^{-/-}$ mice (Jackson Laboratory, 018298), *Irf1*$^{-/-}$ mice (Matsuyama et al., 1993), *Nlrp3*$^{-/-}$ mice (Kanneganti et al., 2006), *Nlrc4*$^{-/-}$ mice (Franchi et al., 2006), *Nlrp3*$^{-/-}$*Nlrc4*$^{-/-}$ mice (generated by crossing *Nlrp3*$^{-/-}$ and *Nlrc4*$^{-/-}$ mice in our facility), *Aim2*$^{-/-}$ mice (Jones et al., 2010b), *Pyrin*$^{-/-}$ mice (Gorp et al., 2016), and *Naip5*$^{-/-}$ mice (kindly provided by Dr. R. Vance), *Il18*$^{-/-}$*Il1r*$^{-/-}$ mice (generated by crossing *Il18*$^{-/-}$ and *Il1r*$^{-/-}$ mice in our facility), *Gsdmd*$^{-/-}$ mice (generated in our facility), *Casp1*$^{-/-}$ mice (Man et al., 2017), *Casp11*$^{-/-}$ mice (Kayagaki et al., 2011), *Irf3*$^{-/-}$ mice (Sato et al., 2000), *Irf7*$^{-/-}$ mice (Honda et al., 2005), *Irf3*$^{-/-}$ *Irf7*$^{-/-}$ mice (generated by crossing *Irf3*$^{-/-}$ and *Irf7*$^{-/-}$ mice in our facility), *Irf9*$^{-/-}$ mice (Kimura et al., 1996), *Ifnar1*$^{-/-}$ mice (Müller et al., 1994), *Ifnar2*$^{-/-}$ mice (Fenner et al., 2006), *Stat1*$^{-/-}$ mice (Matsuyama et al., 1993), *Trif*$^{-/-}$ mice (Yamamoto et al., 2003), *Mavs1*$^{-/-}$ mice (Suthar et al., 2012), *Ifih1*$^{-/-}$ (*Mda5*$^{-/-}$) mice (Kato et al., 2006), *Mb21d1*$^{-/-}$ (*Cgas*$^{-/-}$) mice (Schoggins et al., 2014), and *Tmem173*$^{-/-}$ (*Sting*$^{gt/gt}$) mice (Sauer et al., 2011) have been described. All mice were bred at St. Jude Children's Research Hospital. Animal studies were conducted under protocols approved by St. Jude Children's Research Hospital's committee on the use and care of animals.

Bone Marrow-Derived Macrophages—Primary BMDMs were grown for 6 days in DMEM (ThermoFisher Scientific, 11995-073) supplemented with 1% non-essential amino acids (ThermoFisher Scientific, 11140-050), 10% FBS (Biowest, S1620), 30% medium conditioned by L929 mouse fibroblasts, and 1% penicillin and streptomycin (ThermoFisher Scientific, 15070-063). BMDMs in antibiotic-free medium were seeded onto 12-well plates at a density of 1×10^6 cells per well, followed by incubation overnight.

Bacterial Culture—*F. novicida* strain U112 was grown overnight under aerobic conditions at 37°C in BBL Trypticase Soy Broth (BD Biosciences, 211768) supplemented with 0.2% L-cysteine (ThermoFisher Scientific, BP376-100). Bacteria were subcultured (1:10) for 4 h at 37°C in fresh Trypticase Soy Broth supplemented with 0.2% L-cysteine and resuspended in PBS (ThermoFisher Scientific, 14190-250). *Salmonella* Typhimurium strain SL1344, isogenic mutants lacking *SPI-1* (Δ*SPI-1*), isogenic mutants lacking *SPI-2* (Δ*SPI-2*), isogenic mutants lacking *fliC* and *fljB* (Δ*fliC*Δ*fljB*), *Burkholderia thailandensis* strain E264 (a gift from Dr. Joseph Mougous), and *Pseudomonas aeruginosa* strain PAO1 (a gift from Dr. Joseph Mougous) were inoculated into Luria-Bertani (LB) broth (MP Biomedicals, 3002-031) and incubated overnight under aerobic conditions at 37°C. *S.* Typhimurium SL1344, all isogenic mutants of *S.* Typhimurium SL1344, *B. thailandensis* strain E264, and *P. aeruginosa* strain PAO1 were subcultured (1:10) for 3 h at 37°C in fresh LB broth to generate bacteria grown to log phase. *C. difficile* strain r20291 AB− and AB+ strains were provided by Dr. N. Minton (Kuehne et al., 2014). Strains were streaked onto brain heart infusion agar (BD Biosciences, 211065) and incubated overnight at 37°C in an anaer obic chamber. Single colonies were inoculated into tryptone-yeast extract medium and grown overnight at 37°C anaerobically. *C. difficile* cultures for cell stimulation were prepared by collecting supernatant via centrifugation followed by sterilization through a 0.2 μm filter.

METHODS DETAILS

Stimulation of Bone Marrow–Derived Macrophages—For activation of the canonical NLRP3 inflammasome, BMDMs were primed for 4 h with 100 ng/mL ultrapure LPS from *Salmonella minnesota* R595 (InvivoGen, tlrl-smlps) and were stimulated for 45 min with 5 mM ATP (Roche, 10127531001). For transfection of DNA, each reaction consisted of 2 μg of poly(dA:dT) (InvivoGen, tlrl-patn) resuspended in PBS and mixed with 0.6 μL of Xfect polymer in Xfect reaction buffer (Clontech Laboratories, Inc, 631318). After 10 min, DNA complexes were added to BMDMs in Opti-MEM (ThermoFisher Scientific, 31985-070), followed by incubation for 5 h. For IRF8 expression, BMDMs were stimulated with 100 ng/mL ultrapure LPS for indicated times. For bacterial protein transfection, 0.1 μg, 0.5 μg, or 1 μg of ultrapure flagellin from *Salmonella* Typhimurium (InvivoGen, tlrl-epstfla-5); 1 μg of recombinant *Salmonella* Typhimurium PrgI (Mybiosource, MBS1177087); and 1 μg of recombinant *Salmonella* Typhimurium PrgJ (Mybiosource, MBS2061410) were resuspended in PBS and mixed with 20 μL of DOTAP (Roche, 11202375001) per reaction. The reaction mixture was incubated for 1 h and added to BMDMs in 500 μL Opti-MEM.

For bacterial infection, the following conditions were used: *F. novicida* at an MOI of 100 for 20 h of incubation (for activation of caspase-1) and an MOI of 50 for 2, 8, 16, or 24 h of incubation (for expression of IRF8, GBP2, and GBP5); *S.* Typhimurium at an MOI of 0.01, 0.1, or 1 for 4 h of incubation (for activation of caspase-1) and an MOI of 0.01 for indicated times (for expression of IRF8); Δ*SPI-1* at an MOI of 1 for 4 h of incubation; Δ*SPI-2* at an MOI of 1 for 4 h of incubation; Δ*fliC*Δ*fljB* at an MOI of 1 for 4 h of incubation; *B. thailandensis* at an MOI of 0.5, 1, or 5 for 4 h of incubation (for activation of caspase-1) and an MOI of 1 for indicated times (for expression of IRF8); and *P. aeruginosa* at an MOI of 0.5, 1, or 5 for 4 h of incubation. 50 μg/ml gentamicin (ThermoFisher Scientific, 15750-060)

was added after 8 h (*F. novicida*) post-infection to kill extracellular bacteria. Cell culture supernatants were collected for enzyme-linked immunosorbent assays (ELISAs). Levels of lactate dehydrogenase released by cells were measured by performing a CytoTox 96 non-radioactive cytotoxicity assay according to the manufacturer's instructions (Promega, G1780).

Knockdown via small interfering RNA—BMDMs were transfected for 48 h with small interfering RNA (siRNA) from siGENOME smart pools by using the GenMute siRNA Transfection Reagent according to the manufacturer's instructions (SignaGen Laboratories, SL100568). The siGENOME SMARTpool siRNA specific for mouse *Irf8* (Dharmacon, M-040737-00) was used in the study. A control siRNA pool was also used. Transfected cells were infected with *S.* Typhimurium as described above.

Immunoblot analysis—BMDM cell lysates and culture supernatants were combined in caspase lysis buffer (containing protease inhibitors, phosphatase inhibitors, 10% NP-40, and 25mM DTT) and sample loading buffer (containing SDS and 2-mercaptoethanol) for immunoblot analysis of caspase-1. For immunoblot analysis of signaling, supernatants were removed and BMDMs were washed once with PBS, followed by lysis in RIPA buffer and sample loading buffer (containing SDS and 2-Mercaptoethanol). Proteins were separated by electrophoresis through 8–12% polyacrylamide gels. Following electrophoretic transfer of proteins onto PVDF membranes (Millipore, IPVH00010), nonspecific binding was blocked by incubation with 5% skim milk, then membranes were incubated with primary antibodies anti-caspase-1 (1:3,000 dilution; Adipogen, AG-20B-0042), anti-IRF8 (1:1,000 dilution; Santa Cruz Biotechnology, sc-6058), anti-GBP2 (1:1,000 dilution; Proteintech, 11854-1-AP), anti-GBP5 (1:1,000 dilution; Proteintech, 13220-1-AP), or anti-β-actin (1:10,000 dilution; Proteintech, 66009-1-IG). Membranes were then washed and incubated with the appropriate horseradish peroxidase (HRP)–conjugated secondary antibodies (1:5,000 dilution; Jackson Immuno Research Laboratories, anti-rabbit [111-035-047], anti-mouse [315-035-047], and anti-goat [705-035-003]) for 1 h. Proteins were visualized by using Luminata Forte Western HRP Substrate (Millipore, WBLUF0500).

Real-time (RT-PCR) analysis—For bacterial stimulation, the following conditions were used: *S.* Typhimurium at an MOI of 0.01; and for flagellin transfection, 0.1 μg of flagellin. RNA was extracted by using TRIzol (ThermoFisher Scientific, 15596026) according to the manufacturer's instructions. The isolated RNA was reverse-transcribed into cDNA by using a First-Strand cDNA Synthesis Kit (Applied Biosystems, 4368814). Real-time quantitative PCR was performed on an ABI 7500 RT-PCR instrument by using 2X SYBR Green (Applied Biosystems, 4368706) and the appropriate primers. RT-PCR primer sequences are found in the Key Resources Table.

Cytokine analysis—Cytokines were measured by performing multiplex ELISA (Millipore, MCYTOMAG-70K) or ELISA for IL-18 (Invitrogen, BMS618-3) according to the manufacturer's instructions.

Flow cytometry—The following monoclonal antibodies were used for flow cytometry cellular analyses: CD11b (M1/70; Affymetrix eBioscience, 48-0112-82) and F4/80 (BM8;

BioLegend, 123109). The dilution factor used for these antibodies was 1:300. Flow cytometry data were acquired on a FACSCalibur flow cytometer (BD) and were analyzed by using FlowJo software (FlowJo, LLC and Illumina, Inc).

Microarray, Network analysis, and ChIP-seq—Transcripts were profiled for *S.* Typhimurium-infected BMDMs obtained from WT and *Irf8*$^{-/-}$ mice. Total RNA (100 ng) was converted into biotin-labeled cRNA by using an Ambion Wild-Type Expression kit (ThermoFisher Scientific, 4411973) and was hybridized to a Affymetrix GeneChip Mouse Gene 2.0 ST Array (ThermoFisher Scientific, 902119). After chips were stained and washed, array signals were normalized and transformed into log2 transcript expression values by using the robust multi-array average algorithm (Partek Genomics Suite version 6.6) 49. Differential expression was defined by application of a difference in expression of 0.5-fold (log2 signal) between conditions. Lists of differentially expressed transcripts were analyzed for 'functional enrichment' by using the DAVID bioinformatics database 50 (Huang et al., 2009) and Ingenuity Pathways Analysis software (Qiagen). An interaction network was generated by using the GeneMANIA Cytoscape plugin with default settings (Mostafavi et al., 2008). FASTQ files corresponding to input (GEO Accession number: GSM1721243), IRF8 ChIP (GEO Accession number: GSM1721244) (Olsson et al., 2016) were downloaded from the Sequence Read Archive database by using SRA toolkit. FASTQ files were uploaded to DNA Nexus (St. Jude Cloud), and sequence reads were mapped against the GRCm38/mm10 genome build. Bedgraph files corresponding to IRF4 ChIP-seq experiment were downloaded from GEO database (GEO Accession number: GSE85172) (Iwata et al., 2017). BED files containing the enrichment scores for SPI1 binding were also downloaded from GEO database (GEO Accession number: GSE77886) (Langlais et al., 2016). The result was visualized using Integrative Genomics Viewer (IGV) (Robinson et al., 2011).

ChIP-PCR—WT BMDMs were cross-linked with 1% paraformaldehyde for 10 min followed by glycin quenching. Samples were washed with ice cold PBS and scraped in PBS supplemented with protease inhibitors. Cell pellets were incubated with SDS lysis buffer for 10 min on ice followed by sonication using Covaris sonicator to obtain the desired fragment length (300 bps to 700 bps). An equal amount of DNA was used for IgG (control) (Cell Signaling Technology, 2729) and IRF8 (Cell Signaling Technology, 5628) immunoprecipitation. Immunoprecipitated DNA was eluted in elution buffer and amplified with primers for *Naip2* and *Naip5* (found in Key Resources Table).

Luciferase assay—The *Naip2* and *Naip5* promoter fragments nt −1kb to + 1kb, were amplified by PCR using mouse genomic DNA as a template and inserted into the KpnI and XhoI sites of the luciferase reporter plasmid pGL4.17 basic vector (Promega, E6721) yielding reporter constructs pGL4.17 Naip2 and pGL4.17 Naip5 respectively. HEK293T cells (ATCC, 3216) were co-transfected with the mixture of the indicated luciferase reporter plasmid and pRL-TK-Renilla luciferase (Promega, E2241) plasmid using FuGENE (Promega, E2311) according to manufacturer's instructions. For inducing IRF8 expression, cells were transfected with pCMV6-mIRF8 vector (Origene, MR206748) and luciferase activity was quantified 48 h after transfection with the Dual-Luciferase Reporter Assay

System (Promega, E1910) according to the manufacturer's instructions. pcDNA3.1 (Invitrogen, V79020) was used as empty vector control.

Electrophoretic Mobility Shift Assay—Nuclear extracts from BMDMs were prepared using NP-40 lysis buffer. EMSA was performed using Light Shift Chemiluminescent EMSA kit (ThermoFisher Scientific, 20148). Analysis of IRF8 binding to predicted sites was performed using annealed biotin labeled oligonucleotide probes in a 20μl reaction mixture for 20 min at room temperature. Samples were run on a non-denaturing 5% polyacrylamide gel and transferred to a nylon membrane (ThermoFisher Scientific, 77016), cross-linked in UV. Probes are listed in Key Resources Table.

IRF8 complementation—Primary mouse BMDMs were transfected with the control pcDNA3.1 or pCMV6-mIRF8 vector (Origene, MR206748) by nucleofection (ThermoFisher Scientific, MPK10025) following the manufacturer's instructions.

Animal infection—Frozen stocks of *S.* Typhimurium or *B. thailandensis* were prepared from LB–grown *S.* Typhimurium or *B. thailandensis*, quantified prior to infection, and diluted in PBS for infections. For *S.* Typhimurium infection, mice were injected intraperitoneally with 10^3 CFU in 200 μL PBS. For *B. thailandensis* infection, mice were lightly anesthetized with isoflurane and inoculated intranasally with 5×10^4 CFU in 50 μL PBS. After 3 days of *S.* Typhimurium or 2 days of *B. thailandensis* infection, lungs, liver, and spleen were collected and then homogenized for 2 min in PBS with metal beads by using a TissueLyser II apparatus (Qiagen). CFU values were quantified by plating lysates onto LB agar, followed by incubation overnight. No randomization or blinding was used. Formalin preserved lungs were processed and embedded in paraffin according to standard procedures. Sections (5 μm) were stained with H&E and examined.

QUANTIFICATION AND STATISTICAL ANALYSIS

Statistical analysis—GraphPad Prism 6.0 software was used for data analysis. Data are shown as mean ± SEM. Statistical significance was determined by *t* tests (two-tailed) for two groups or ANOVA (with Dunnett's multiple comparisons test, Dunn's multiple comparisons test, or Tukey's multiple comparisons test) for three or more groups. Survival curves were compared with the log-rank test outcome. *P* values less than 0.05 were considered to be statistically significant.

DATA RESOURCES

Microarray—The dataset was deposited under the accession code GSE110452.

Supplementary Material

Refer to Web version on PubMed Central for supplementary material.

Acknowledgments

We thank A. Burton from St. Jude Children's Research Hospital for technical support. We thank members of the Kanneganti laboratory for their comments and suggestions. Work from our laboratory is supported by the US

National Institutes of Health (AI101935, AI124346, AR056296 and CA163507 to T.-D.K.), and the American Lebanese Syrian Associated Charities (to T.-D.K.)

References

Amer A, Franchi L, Kanneganti TD, Body-Malapel M, Özören N, Brady G, Meshinchi S, Jagirdar R, Gewirtz A, Akira S, et al. Regulation of Legionella Phagosome Maturation and Infection through Flagellin and Host Ipaf. J Biol Chem. 2006; 281:35217–35223. [PubMed: 16984919]

Barber SA, Fultz MJ, Salkowski CA, Vogel SN. Differential expression of interferon regulatory factor 1 (IRF-1), IRF-2, and interferon consensus sequence binding protein genes in lipopolysaccharide (LPS)-responsive and LPS-hyporesponsive macrophages. Infect Immun. 1995; 63:601–608. [PubMed: 7822029]

Bovolenta C, Driggers PH, Marks MS, Medin JA, Politis AD, Vogel SN, Levy DE, Sakaguchi K, Appella E, Coligan JE. Molecular interactions between interferon consensus sequence binding protein and members of the interferon regulatory factor family. Proc Natl Acad Sci U S A. 1994; 91:5046–5050. [PubMed: 8197182]

Broz P, Newton K, Lamkanfi M, Mariathasan S, Dixit VM, Monack DM. Redundant roles for inflammasome receptors NLRP3 and NLRC4 in host defense against Salmonella. J Exp Med. 2010; 207:1745–1755. [PubMed: 20603313]

Broz P, Ruby T, Belhocine K, Bouley DM, Kayagaki N, Dixit VM, Monack DM. Caspase-11 increases susceptibility to Salmonella infection in the absence of caspase-1. Nature. 2012; 490:288–291. [PubMed: 22895188]

Carvalho FA, Nalbantoglu I, Aitken JD, Uchiyama R, Su Y, Doho GH, Vijay-Kumar M, Gewirtz AT. Cytosolic flagellin receptor NLRC4 protects mice against mucosal and systemic challenges. Mucosal Immunol. 2012; 5:288–298. [PubMed: 22318495]

Crowley SM, Knodler LA, Vallance BA. Salmonella and the Inflammasome: Battle for Intracellular Dominance. Curr Top Microbiol Immunol. 2016; 397:43–67. [PubMed: 27460804]

Driggers PH, Ennist DL, Gleason SL, Mak WH, Marks MS, Levi BZ, Flanagan JR, Appella E, Ozato K. An interferon gamma-regulated protein that binds the interferon-inducible enhancer element of major histocompatibility complex class I genes. Proc Natl Acad Sci. 1990; 87:3743–3747. [PubMed: 2111015]

Eklund EA, Jalava A, Kakar R. PU. 1, Interferon Regulatory Factor 1, and Interferon Consensus Sequence-binding Protein Cooperate to Increase gp91 phox Expression. J Biol Chem. 1998; 273:13957–13965. [PubMed: 9593745]

Fàbrega A, Vila J. Salmonella enterica Serovar Typhimurium Skills To Succeed in the Host: Virulence and Regulation. Clin Microbiol Rev. 2013; 26:308–341. [PubMed: 23554419]

Fenner JE, Starr R, Cornish AL, Zhang JG, Metcalf D, Schreiber RD, Sheehan K, Hilton DJ, Alexander WS, Hertzog PJ. Suppressor of cytokine signaling 1 regulates the immune response to infection by a unique inhibition of type I interferon activity. Nat Immunol. 2006; 7:33–39. [PubMed: 16311601]

Fernandes-Alnemri T, Yu JW, Juliana C, Solorzano L, Kang S, Wu J, Datta P, McCormick M, Huang L, McDermott E, et al. The AIM2 inflammasome is critical for innate immunity to Francisella tularensis. Nat Immunol. 2010; 11:385–393. [PubMed: 20351693]

Franchi L, Amer A, Body-Malapel M, Kanneganti TD, Özören N, Jagirdar R, Inohara N, Vandenabeele P, Bertin J, Coyle A, et al. Cytosolic flagellin requires Ipaf for activation of caspase-1 and interleukin 1β in salmonella-infected macrophages. Nat Immunol. 2006; 7:576–582. [PubMed: 16648852]

Fujita T, Kimura Y, Miyamoto M, Barsoumian EL, Taniguchi T. Induction of endogenous IFN-α and IFN-β genes by a regulatory transcription factor, IRF-1. Nature. 1989; 337:270–272. [PubMed: 2911367]

Glasmacher E, Agrawal S, Chang AB, Murphy TL, Zeng W, Lugt BV, Khan AA, Ciofani M, Spooner CJ, Rutz S, et al. A Genomic Regulatory Element That Directs Assembly and Function of Immune-Specific AP-1–IRF Complexes. Science. 2012; 338:975–980. [PubMed: 22983707]

Gorp HV, Saavedra PHV, de Vasconcelos NM, Opdenbosch NV, Walle LV, Matusiak M, Prencipe G, Insalaco A, Hauwermeiren FV, Demon D, et al. Familial Mediterranean fever mutations lift the

obligatory requirement for microtubules in Pyrin inflammasome activation. Proc Natl Acad Sci. 2016; 113:14384–14389. [PubMed: 27911804]

Harada H, Fujita T, Miyamoto M, Kimura Y, Maruyama M, Furia A, Miyata T, Taniguchi T. Structurally similar but functionally distinct factors, IRF-1 and IRF-2, bind to the same regulatory elements of IFN and IFN-inducible genes. Cell. 1989; 58:729–739. [PubMed: 2475256]

Henry T, Brotcke A, Weiss DS, Thompson LJ, Monack DM. Type I interferon signaling is required for activation of the inflammasome during Francisella infection. J Exp Med. 2007; 204:987–994. [PubMed: 17452523]

Honda K, Yanai H, Negishi H, Asagiri M, Sato M, Mizutani T, Shimada N, Ohba Y, Takaoka A, Yoshida N, et al. IRF-7 is the master regulator of type-I interferon-dependent immune responses. Nature. 2005; 434:772–777. [PubMed: 15800576]

Huang DW, Sherman BT, Lempicki RA. Systematic and integrative analysis of large gene lists using DAVID bioinformatics resources. Nat Protoc. 2009; 4:44–57. [PubMed: 19131956]

Ivashkiv LB, Donlin LT. Regulation of type I interferon responses. Nat Rev Immunol. 2014; 14:36–49. [PubMed: 24362405]

Iwata A, Durai V, Tussiwand R, Briseño CG, Wu X, Grajales-Reyes GE, Egawa T, Murphy TL, Murphy KM. Quality of TCR signaling determined by differential affinities of enhancers for the composite BATF-IRF4 transcription factor complex. Nat Immunol. 2017; 18:563–572. [PubMed: 28346410]

Jones CL, Napier BA, Sampson TR, Llewellyn AC, Schroeder MR, Weiss DS. Subversion of Host Recognition and Defense Systems by Francisella spp. Microbiol Mol Biol Rev. 2012; 76:383–404. [PubMed: 22688817]

Jones JDG, Vance RE, Dangl JL. Intracellular innate immune surveillance devices in plants and animals. Science. 2016; 354:aaf6395. [PubMed: 27934708]

Jones JW, Kayagaki N, Broz P, Henry T, Newton K, O'Rourke K, Chan S, Dong J, Qu Y, Roose-Girma M, et al. Absent in melanoma 2 is required for innate immune recognition of Francisella tularensis. Proc Natl Acad Sci. 2010a; 107:9771–9776. [PubMed: 20457908]

Jones JW, Kayagaki N, Broz P, Henry T, Newton K, O'Rourke K, Chan S, Dong J, Qu Y, Roose-Girma M, et al. Absent in melanoma 2 is required for innate immune recognition of Francisella tularensis. Proc Natl Acad Sci. 2010b; 107:9771–9776. [PubMed: 20457908]

Kanneganti TD, Özören N, Body-Malapel M, Amer A, Park JH, Franchi L, Whitfield J, Barchet W, Colonna M, Vandenabeele P, et al. Bacterial RNA and small antiviral compounds activate caspase-1 through cryopyrin/Nalp3. Nature. 2006; 440:233–236. [PubMed: 16407888]

Kato H, Takeuchi O, Sato S, Yoneyama M, Yamamoto M, Matsui K, Uematsu S, Jung A, Kawai T, Ishii KJ, et al. Differential roles of MDA5 and RIG-I helicases in the recognition of RNA viruses. Nature. 2006; 441:101–105. [PubMed: 16625202]

Kayagaki N, Warming S, Lamkanfi M, Vande Walle L, Louie S, Dong J, Newton K, Qu Y, Liu J, Heldens S, et al. Non-canonical inflammasome activation targets caspase-11. Nature. 2011; 479:117–121. [PubMed: 22002608]

Kayagaki N, Stowe IB, Lee BL, O'Rourke K, Anderson K, Warming S, Cuellar T, Haley B, Roose-Girma M, Phung QT, et al. Caspase-11 cleaves gasdermin D for non-canonical inflammasome signalling. Nature. 2015; 526:666–671. [PubMed: 26375259]

Kimura T, Kadokawa Y, Harada H, Matsumoto M, Sato M, Kashiwazaki Y, Tarutani M, Tan RS, Takasugi T, Matsuyama T, et al. Essential and non-redundant roles of p48 (ISGF3 gamma) and IRF-1 in both type I and type II interferon responses, as revealed by gene targeting studies. Genes Cells Devoted Mol Cell Mech. 1996; 1:115–124.

Kofoed EM, Vance RE. Innate immune recognition of bacterial ligands by NAIPs determines inflammasome specificity. Nature. 2011; 477:592–595. [PubMed: 21874021]

Kortmann J, Brubaker SW, Monack DM. Cutting Edge: Inflammasome Activation in Primary Human Macrophages Is Dependent on Flagellin. J Immunol. 2015; 195:815–819. [PubMed: 26109648]

Kuehne SA, Collery MM, Kelly ML, Cartman ST, Cockayne A, Minton NP. Importance of Toxin A, Toxin B, and CDT in Virulence of an Epidemic Clostridium difficile Strain. J Infect Dis. 2014; 209:83–86. [PubMed: 23935202]

Kurotaki D, Tamura T. Transcriptional and Epigenetic Regulation of Innate Immune Cell Development by the Transcription Factor, Interferon Regulatory Factor-8. J Interferon Cytokine Res. 2016; 36:433–441. [PubMed: 27379865]

Langlais D, Barreiro LB, Gros P. The macrophage IRF8/IRF1 regulome is required for protection against infections and is associated with chronic inflammation. J Exp Med. 2016; 213:585–603. [PubMed: 27001747]

Lehtonen A, Matikainen S, Julkunen I. Interferons up-regulate STAT1, STAT2, and IRF family transcription factor gene expression in human peripheral blood mononuclear cells and macrophages. J Immunol. 1997; 159:794–803. [PubMed: 9218597]

Liu J, Guan X, Tamura T, Ozato K, Ma X. Synergistic Activation of Interleukin-12 p35 Gene Transcription by Interferon Regulatory Factor-1 and Interferon Consensus Sequence-binding Protein. J Biol Chem. 2004; 279:55609–55617. [PubMed: 15489234]

Liu X, Zhang Z, Ruan J, Pan Y, Magupalli VG, Wu H, Lieberman J. Inflammasome-activated gasdermin D causes pyroptosis by forming membrane pores. Nature. 2016; 535:153. [PubMed: 27383986]

Man SM, Kanneganti TD. Regulation of inflammasome activation. Immunol Rev. 2015; 265:6–21. [PubMed: 25879280]

Man SM, Hopkins LJ, Nugent E, Cox S, Glück IM, Tourlomousis P, Wright JA, Cicuta P, Monie TP, Bryant CE. Inflammasome activation causes dual recruitment of NLRC4 and NLRP3 to the same macromolecular complex. Proc Natl Acad Sci. 2014; 111:7403–7408. [PubMed: 24803432]

Man SM, Karki R, Malireddi RKS, Neale G, Vogel P, Yamamoto M, Lamkanfi M, Kanneganti TD. The transcription factor IRF1 and guanylate-binding proteins target activation of the AIM2 inflammasome by Francisella infection. Nat Immunol. 2015; 16:467–475. [PubMed: 25774715]

Man SM, Karki R, Briard B, Burton A, Gingras S, Pelletier S, Kanneganti T-D. Differential roles of caspase-1 and caspase-11 in infection and inflammation. Sci Rep. 2017; 7:srep45126.

Mariathasan S, Newton K, Monack DM, Vucic D, French DM, Lee WP, Roose-Girma M, Erickson S, Dixit VM. Differential activation of the inflammasome by caspase-1 adaptors ASC and Ipaf. Nature. 2004; 430:213–218. [PubMed: 15190255]

Martone R, Euskirchen G, Bertone P, Hartman S, Royce TE, Luscombe NM, Rinn JL, Nelson FK, Miller P, Gerstein M, et al. Distribution of NF-κB-binding sites across human chromosome 22. Proc Natl Acad Sci. 2003; 100:12247–12252. [PubMed: 14527995]

Masumi A, Tamaoki S, Wang IM, Ozato K, Komuro K. IRF-8/ICSBP and IRF-1 cooperatively stimulate mouse IL-12 promoter activity in macrophages. FEBS Lett. 2002; 531:348–353. [PubMed: 12417340]

Matsuyama T, Kimura T, Kitagawa M, Pfeffer K, Kawakami T, Watanabe N, Kündig TM, Amakawa R, Kishihara K, Wakeham A, et al. Targeted disruption of IRF-1 or IRF-2 results in abnormal type I IFN gene induction and aberrant lymphocyte development. Cell. 1993; 75:83–97. [PubMed: 8402903]

Miao EA, Alpuche-Aranda CM, Dors M, Clark AE, Bader MW, Miller SI, Aderem A. Cytoplasmic flagellin activates caspase-1 and secretion of interleukin 1β via Ipaf. Nat Immunol. 2006; 7:569–575. [PubMed: 16648853]

Mostafavi S, Ray D, Warde-Farley D, Grouios C, Morris Q. GeneMANIA: a real-time multiple association network integration algorithm for predicting gene function. Genome Biol. 2008; 9:S4.

Müller U, Steinhoff U, Reis LF, Hemmi S, Pavlovic J, Zinkernagel RM, Aguet M. Functional role of type I and type II interferons in antiviral defense. Science. 1994; 264:1918–1921. [PubMed: 8009221]

Olsson A, Venkatasubramanian M, Chaudhri VK, Aronow BJ, Salomonis N, Singh H, Grimes HL. Single-cell analysis of mixed-lineage states leading to a binary cell fate choice. Nature. 2016; 537:698–702. [PubMed: 27580035]

Rathinam VAK, Vanaja SK, Waggoner L, Sokolovska A, Becker C, Stuart LM, Leong JM, Fitzgerald KA. TRIF Licenses Caspase-11-Dependent NLRP3 Inflammasome Activation by Gram-Negative Bacteria. Cell. 2012; 150:606–619. [PubMed: 22819539]

Rauch I, Tenthorey JL, Nichols RD, Moussawi KA, Kang JJ, Kang C, Kazmierczak BI, Vance RE. NAIP proteins are required for cytosolic detection of specific bacterial ligands in vivo. J Exp Med. 2016; 213:657–665. [PubMed: 27045008]

Robinson JT, Thorvaldsdóttir H, Winckler W, Guttman M, Lander ES, Getz G, Mesirov JP. Integrative genomics viewer. Nat Biotechnol. 2011; 29:24–26. [PubMed: 21221095]

Sato M, Suemori H, Hata N, Asagiri M, Ogasawara K, Nakao K, Nakaya T, Katsuki M, Noguchi S, Tanaka N, et al. Distinct and Essential Roles of Transcription Factors IRF-3 and IRF-7 in Response to Viruses for IFN-α/β Gene Induction. Immunity. 2000; 13:539–548. [PubMed: 11070172]

Sauer JD, Sotelo-Troha K, von Moltke J, Monroe KM, Rae CS, Brubaker SW, Hyodo M, Hayakawa Y, Woodward JJ, Portnoy DA, et al. The N-ethyl-N-nitrosourea-induced Goldenticket mouse mutant reveals an essential function of Sting in the in vivo interferon response to Listeria monocytogenes and cyclic dinucleotides. Infect Immun. 2011; 79:688–694. [PubMed: 21098106]

Schoggins JW, MacDuff DA, Imanaka N, Gainey MD, Shrestha B, Eitson JL, Mar KB, Richardson RB, Ratushny AV, Litvak V, et al. Pan-viral specificity of IFN-induced genes reveals new roles for cGAS in innate immunity. Nature. 2014; 505:691–695. [PubMed: 24284630]

Sellin ME, Müller AA, Felmy B, Dolowschiak T, Diard M, Tardivel A, Maslowski KM, Hardt WD. Epithelium-Intrinsic NAIP/NLRC4 Inflammasome Drives Infected Enterocyte Expulsion to Restrict Salmonella Replication in the Intestinal Mucosa. Cell Host Microbe. 2014; 16:237–248. [PubMed: 25121751]

Shi J, Zhao Y, Wang K, Shi X, Wang Y, Huang H, Zhuang Y, Cai T, Wang F, Shao F. Cleavage of GSDMD by inflammatory caspases determines pyroptotic cell death. Nature. 2015; 526:660–665. [PubMed: 26375003]

Sichien D, Scott CL, Martens L, Vanderkerken M, Van Gassen S, Plantinga M, Joeris T, De Prijck S, Vanhoutte L, Vanheerswynghels M, et al. IRF8 Transcription Factor Controls Survival and Function of Terminally Differentiated Conventional and Plasmacytoid Dendritic Cells, Respectively. Immunity. 2016; 45:626–640. [PubMed: 27637148]

Storek KM, Monack DM. Bacterial recognition pathways that lead to inflammasome activation. Immunol Rev. 2015; 265:112–129. [PubMed: 25879288]

Suthar MS, Ramos HJ, Brassil MM, Netland J, Chappell CP, Blahnik G, McMillan A, Diamond MS, Clark EA, Bevan MJ, et al. The RIG-I-like receptor LGP2 controls CD8(+) T cell survival and fitness. Immunity. 2012; 37:235–248. [PubMed: 22841161]

Sutterwala FS, Mijares LA, Li L, Ogura Y, Kazmierczak BI, Flavell RA. Immune recognition of Pseudomonas aeruginosa mediated by the IPAF/NLRC4 inflammasome. J Exp Med. 2007; 204:3235–3245. [PubMed: 18070936]

Tailor P, Tamura T, Kong HJ, Kubota T, Kubota M, Borghi P, Gabriele L, Ozato K. The Feedback Phase of Type I Interferon Induction in Dendritic Cells Requires Interferon Regulatory Factor 8. Immunity. 2007; 27:228–239. [PubMed: 17702615]

Tamura T, Yanai H, Savitsky D, Taniguchi T. The IRF family transcription factors in immunity and oncogenesis. Annu Rev Immunol. 2008; 26:535–584. [PubMed: 18303999]

Tokuhiro S, Yamada R, Chang X, Suzuki A, Kochi Y, Sawada T, Suzuki M, Nagasaki M, Ohtsuki M, Ono M, et al. An intronic SNP in a RUNX1 binding site of SLC22A4, encoding an organic cation transporter, is associated with rheumatoid arthritis. Nat Genet. 2003; 35:341–348. [PubMed: 14608356]

Veals SA, Schindler C, Leonard D, Fu XY, Aebersold R, Darnell JE, Levy DE. Subunit of an alpha-interferon-responsive transcription factor is related to interferon regulatory factor and Myb families of DNA-binding proteins. Mol Cell Biol. 1992; 12:3315–3324. [PubMed: 1630447]

Wang IM, Contursi C, Masumi A, Ma X, Trinchieri G, Ozato K. An IFN-γ-Inducible Transcription Factor, IFN Consensus Sequence Binding Protein (ICSBP), Stimulates IL-12 p40 Expression in Macrophages. J Immunol. 2000; 165:271–279. [PubMed: 10861061]

Wei CL, Wu Q, Vega VB, Chiu KP, Ng P, Zhang T, Shahab A, Yong HC, Fu Y, Weng Z, et al. A Global Map of p53 Transcription-Factor Binding Sites in the Human Genome. Cell. 2006; 124:207–219. [PubMed: 16413492]

Xiong H, Zhu C, Li H, Chen F, Mayer L, Ozato K, Unkeless JC, Plevy SE. Complex Formation of the Interferon (IFN) Consensus Sequence-binding Protein with IRF-1 Is Essential for Murine Macrophage IFN-γ-induced iNOS Gene Expression. J Biol Chem. 2003; 278:2271–2277. [PubMed: 12429737]

Xu H, Yang J, Gao W, Li L, Li P, Zhang L, Gong YN, Peng X, Xi JJ, Chen S, et al. Innate immune sensing of bacterial modifications of Rho GTPases by the Pyrin inflammasome. Nature. 2014; 513:237–241. [PubMed: 24919149]

Yamagata T, Nishida J, Tanaka S, Sakai R, Mitani K, Yoshida M, Taniguchi T, Yazaki Y, Hirai H. A novel interferon regulatory factor family transcription factor, ICSAT/Pip/LSIRF, that negatively regulates the activity of interferon-regulated genes. Mol Cell Biol. 1996; 16:1283–1294. [PubMed: 8657101]

Yamamoto M, Sato S, Hemmi H, Hoshino K, Kaisho T, Sanjo H, Takeuchi O, Sugiyama M, Okabe M, Takeda K, et al. Role of adaptor TRIF in the MyD88-independent toll-like receptor signaling pathway. Science. 2003; 301:640–643. [PubMed: 12855817]

Yang J, Zhao Y, Shi J, Shao F. Human NAIP and mouse NAIP1 recognize bacterial type III secretion needle protein for inflammasome activation. Proc Natl Acad Sci. 2013; 110:14408–14413. [PubMed: 23940371]

Zamboni DS, Kobayashi KS, Kohlsdorf T, Ogura Y, Long EM, Vance RE, Kuida K, Mariathasan S, Dixit VM, Flavell RA, et al. The Birc1e cytosolic pattern-recognition receptor contributes to the detection and control of Legionella pneumophila infection. Nat Immunol. 2006; 7:318–325. [PubMed: 16444259]

Zhao Y, Shao F. The NAIP–NLRC4 inflammasome in innate immune detection of bacterial flagellin and type III secretion apparatus. Immunol Rev. 2015; 265:85–102. [PubMed: 25879286]

Zhao Y, Yang J, Shi J, Gong YN, Lu Q, Xu H, Liu L, Shao F. The NLRC4 inflammasome receptors for bacterial flagellin and type III secretion apparatus. Nature. 2011; 477:596–600. [PubMed: 21918512]

Zhao Y, Shi J, Shi X, Wang Y, Wang F, Shao F. Genetic functions of the NAIP family of inflammasome receptors for bacterial ligands in mice. J Exp Med. 2016; 213:647–656. [PubMed: 27114610]

Zitvogel L, Galluzzi L, Kepp O, Smyth MJ, Kroemer G. Type I interferons in anticancer immunity. Nat Rev Immunol. 2015; 15:405–414. [PubMed: 26027717]

References

Broz P, Newton K, Lamkanfi M, Mariathasan S, Dixit VM, Monack DM. Redundant roles for inflammasome receptors NLRP3 and NLRC4 in host defense against Salmonella. J Exp Med. 2010; 207:1745–1755. [PubMed: 20603313]

Edgar R, Domrachev M, Lash AE. Gene Expression Omnibus: NCBI gene expression and hybridization array data repository. Nucleic Acids Res. 2002; 30:207–210. [PubMed: 11752295]

Fenner JE, Starr R, Cornish AL, Zhang JG, Metcalf D, Schreiber RD, Sheehan K, Hilton DJ, Alexander WS, Hertzog PJ. Suppressor of cytokine signaling 1 regulates the immune response to infection by a unique inhibition of type I interferon activity. Nat Immunol. 2006; 7:33–39. [PubMed: 16311601]

Franchi L, Amer A, Body-Malapel M, Kanneganti TD, Özören N, Jagirdar R, Inohara N, Vandenabeele P, Bertin J, Coyle A, et al. Cytosolic flagellin requires Ipaf for activation of caspase-1 and interleukin 1β in salmonella-infected macrophages. Nat Immunol. 2006; 7:576–582. [PubMed: 16648852]

Glaccum MB, Stocking KL, Charrier K, Smith JL, Willis CR, Maliszewski C, Livingston DJ, Peschon JJ, Morrissey PJ. Phenotypic and functional characterization of mice that lack the type I receptor for IL-1. J Immunol Baltim Md 1950. 1997; 159:3364–3371.

Gorp HV, Saavedra PHV, de Vasconcelos NM, Opdenbosch NV, Walle LV, Matusiak M, Prencipe G, Insalaco A, Hauwermeiren FV, Demon D, et al. Familial Mediterranean fever mutations lift the obligatory requirement for microtubules in Pyrin inflammasome activation. Proc Natl Acad Sci. 2016; 113:14384–14389. [PubMed: 27911804]

Honda K, Yanai H, Negishi H, Asagiri M, Sato M, Mizutani T, Shimada N, Ohba Y, Takaoka A, Yoshida N, et al. IRF-7 is the master regulator of type-I interferon-dependent immune responses. Nature. 2005; 434:772–777. [PubMed: 15800576]

Hood RD, Singh P, Hsu F, Güvener T, Carl MA, Trinidad RRS, Silverman JM, Ohlson BB, Hicks KG, Plemel RL, et al. A Type VI Secretion System of Pseudomonas aeruginosa Targets a Toxin to Bacteria. Cell Host Microbe. 2010; 7:25–37. [PubMed: 20114026]

Huang DW, Sherman BT, Lempicki RA. Systematic and integrative analysis of large gene lists using DAVID bioinformatics resources. Nat Protoc. 2009; 4:44–57. [PubMed: 19131956]

Jones JW, Kayagaki N, Broz P, Henry T, Newton K, O'Rourke K, Chan S, Dong J, Qu Y, Roose-Girma M, et al. Absent in melanoma 2 is required for innate immune recognition of Francisella tularensis. Proc Natl Acad Sci. 2010; 107:9771–9776. [PubMed: 20457908]

Kanneganti TD, Özören N, Body-Malapel M, Amer A, Park JH, Franchi L, Whitfield J, Barchet W, Colonna M, Vandenabeele P, et al. Bacterial RNA and small antiviral compounds activate caspase-1 through cryopyrin/Nalp3. Nature. 2006; 440:233–236. [PubMed: 16407888]

Kato H, Takeuchi O, Sato S, Yoneyama M, Yamamoto M, Matsui K, Uematsu S, Jung A, Kawai T, Ishii KJ, et al. Differential roles of MDA5 and RIG-I helicases in the recognition of RNA viruses. Nature. 2006; 441:101–105. [PubMed: 16625202]

Kayagaki N, Warming S, Lamkanfi M, Vande Walle L, Louie S, Dong J, Newton K, Qu Y, Liu J, Heldens S, et al. Non-canonical inflammasome activation targets caspase-11. Nature. 2011; 479:117–121. [PubMed: 22002608]

Kimura T, Kadokawa Y, Harada H, Matsumoto M, Sato M, Kashiwazaki Y, Tarutani M, Tan RS, Takasugi T, Matsuyama T, et al. Essential and non-redundant roles of p48 (ISGF3 gamma) and IRF-1 in both type I and type II interferon responses, as revealed by gene targeting studies. Genes Cells Devoted Mol Cell Mech. 1996; 1:115–124.

Lightfield KL, Persson J, Brubaker SW, Witte CE, von Moltke J, Dunipace EA, Henry T, Sun YH, Cado D, Dietrich WF, et al. Critical function for Naip5 in inflammasome activation by a conserved carboxy-terminal domain of flagellin. Nat Immunol. 2008; 9:1171–1178. [PubMed: 18724372]

Man SM, Karki R, Malireddi RKS, Neale G, Vogel P, Yamamoto M, Lamkanfi M, Kanneganti TD. The transcription factor IRF1 and guanylate-binding proteins target activation of the AIM2 inflammasome by Francisella infection. Nat Immunol. 2015; 16:467–475. [PubMed: 25774715]

Man SM, Karki R, Briard B, Burton A, Gingras S, Pelletier S, Kanneganti T-D. Differential roles of caspase-1 and caspase-11 in infection and inflammation. Sci Rep. 2017; 7:srep45126.

Matsuyama T, Kimura T, Kitagawa M, Pfeffer K, Kawakami T, Watanabe N, Kündig TM, Amakawa R, Kishihara K, Wakeham A, et al. Targeted disruption of IRF-1 or IRF-2 results in abnormal type I IFN gene induction and aberrant lymphocyte development. Cell. 1993; 75:83–97. [PubMed: 8402903]

Mostafavi S, Ray D, Warde-Farley D, Grouios C, Morris Q. GeneMANIA: a real-time multiple association network integration algorithm for predicting gene function. Genome Biol. 2008; 9:S4.

Müller U, Steinhoff U, Reis LF, Hemmi S, Pavlovic J, Zinkernagel RM, Aguet M. Functional role of type I and type II interferons in antiviral defense. Science. 1994; 264:1918–1921. [PubMed: 8009221]

Sato M, Suemori H, Hata N, Asagiri M, Ogasawara K, Nakao K, Nakaya T, Katsuki M, Noguchi S, Tanaka N, et al. Distinct and Essential Roles of Transcription Factors IRF-3 and IRF-7 in Response to Viruses for IFN-α/β Gene Induction. Immunity. 2000; 13:539–548. [PubMed: 11070172]

Sauer JD, Sotelo-Troha K, von Moltke J, Monroe KM, Rae CS, Brubaker SW, Hyodo M, Hayakawa Y, Woodward JJ, Portnoy DA, et al. The N-ethyl-N-nitrosourea-induced Goldenticket mouse mutant reveals an essential function of Sting in the in vivo interferon response to Listeria monocytogenes and cyclic dinucleotides. Infect Immun. 2011; 79:688–694. [PubMed: 21098106]

Schoggins JW, MacDuff DA, Imanaka N, Gainey MD, Shrestha B, Eitson JL, Mar KB, Richardson RB, Ratushny AV, Litvak V, et al. Pan-viral specificity of IFN-induced genes reveals new roles for cGAS in innate immunity. Nature. 2014; 505:691–695. [PubMed: 24284630]

Schwarz S, West TE, Boyer F, Chiang WC, Carl MA, Hood RD, Rohmer L, Tolker-Nielsen T, Skerrett SJ, Mougous JD. Burkholderia Type VI Secretion Systems Have Distinct Roles in Eukaryotic and Bacterial Cell Interactions. PLOS Pathog. 2010; 6:e1001068. [PubMed: 20865170]

Shannon P, Markiel A, Ozier O, Baliga NS, Wang JT, Ramage D, Amin N, Schwikowski B, Ideker T. Cytoscape: a software environment for integrated models of biomolecular interaction networks. Genome Res. 2003; 13:2498–2504. [PubMed: 14597658]

Suthar MS, Ramos HJ, Brassil MM, Netland J, Chappell CP, Blahnik G, McMillan A, Diamond MS, Clark EA, Bevan MJ, et al. The RIG-I-like receptor LGP2 controls CD8(+) T cell survival and fitness. Immunity. 2012; 37:235–248. [PubMed: 22841161]

Takeda K, Tsutsui H, Yoshimoto T, Adachi O, Yoshida N, Kishimoto T, Okamura H, Nakanishi K, Akira S. Defective NK cell activity and Th1 response in IL-18-deficient mice. Immunity. 1998; 8:383–390. [PubMed: 9529155]

Trapnell C, Roberts A, Goff L, Pertea G, Kim D, Kelley DR, Pimentel H, Salzberg SL, Rinn JL, Pachter L. Differential gene and transcript expression analysis of RNA-seq experiments with TopHat and Cufflinks. Nat Protoc. 2012; 7:562–578. [PubMed: 22383036]

Yamamoto M, Sato S, Hemmi H, Hoshino K, Kaisho T, Sanjo H, Takeuchi O, Sugiyama M, Okabe M, Takeda K, et al. Role of adaptor TRIF in the MyD88-independent toll-like receptor signaling pathway. Science. 2003; 301:640–643. [PubMed: 12855817]

Zhang Y, Liu T, Meyer CA, Eeckhoute J, Johnson DS, Bernstein BE, Nusbaum C, Myers RM, Brown M, Li W, et al. Model-based analysis of ChIP-Seq (MACS). Genome Biol. 2008; 9:R137. [PubMed: 18798982]

HIGHLIGHTS

- IRF8 is required for the optimal activation of NLRC4 inflammasome.
- The expression of *Naip1*, *Naip2*, *Naip5*, and *Naip6* is dependent on IRF8.
- IRF8 is dispensable for the activation of NLRP3, AIM2 and Pyrin inflammasomes.
- *Irf8*$^{-/-}$ mice are susceptible to *S.* Typhimurium and *B. thailandensis* infection.

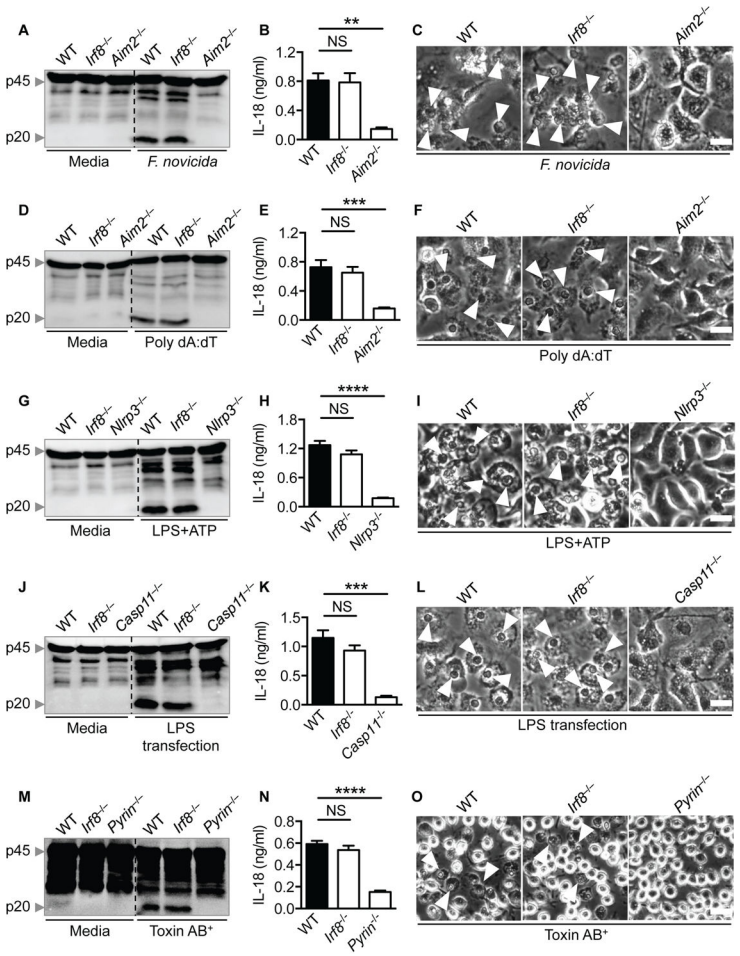

Figure 1. IRF8 does not affect the activation of AIM2, NLRP3, or Pyrin inflammasomes

(**A**) Immunoblot analysis of pro-caspase-1 (p45) and the cleaved caspase-1 (p20) in WT or mutant BMDMs left untreated/uninfected (Media) or infected with *F. novicida* (multiplicity of infection [MOI], 100) and collected after 20 h.

(**B**) Assessment of IL-18 release by enzyme-linked immunosorbent assay (ELISA) following *F. novicida* infection.

(**C**) Images of BMDMs under light microscopy after *F. novicida* infection. The arrows indicate pyroptotic cells.

(**D–F**) Immunoblot analysis of caspase-1, IL-18 release, and cell images of BMDMs after transfection with poly(dA:dT).

(**G–I**) Immunoblot analysis of caspase-1, IL-18 release, and cell images of LPS-primed BMDMs stimulated with ATP.

(**J–L**) Immunoblot analysis of caspase-1, IL-18 release, and cell images of BMDMs primed with LPS and followed by LPS transfection.

(**M–O**) Immunoblot analysis of caspase-1, IL-18 release, and cell images of BMDMs following treatment of toxin from *C. difficile* AB+ strain.

Scale bars, 100 μm (C, F, I, L and O), NS, not significant; $^{**}P < 0.01$, $^{***}P < 0.001$ and $^{****}P < 0.0001$ (One-way ANOVA with Dunnett's multiple comparisons test). Data are

representative of 3 (**A, C, D, F, G, I, J, L, M, and O**) or from 3 (**B, E, H, K, and N**) independent experiments (mean ± SEM).

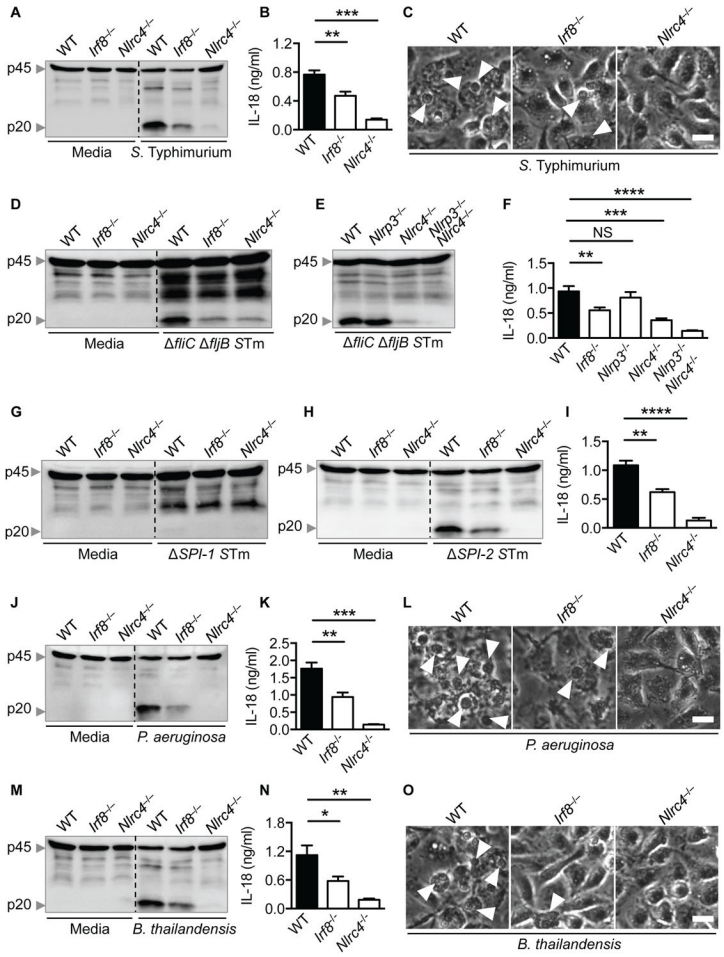

Figure 2. IRF8 is necessary for NLRC4 inflammasome activation induced by bacterial infection

(**A–C**) Immunoblot analysis of caspase-1, IL-18 release, and cell images of BMDMs that were infected with *S.* Typhimurium (MOI, 0.1) and collected after 4 h.

(**D and E**) Immunoblot analysis of caspase-1 in BMDMs that were infected with Δ*fliC*Δ*fljB S.* Typhimurium (Δ*fliC*Δ*fljB*) (MOI, 1) and collected after 4 h.

(**F**) Assessment of IL-18 levels in cell supernatants following Δ*fliC*Δ*fljB* infection.

(**G**) Immunoblot analysis of caspase-1 in BMDMs that were infected with Δ*SPI-1 S.* Typhimurium (Δ*SPI-1*) (MOI, 1) and collected after 4 h.

(**H**) Immunoblot analysis of caspase-1 in BMDMs that were infected with Δ*SPI-2 S.* Typhimurium (Δ*SPI-2*) (MOI, 1) and collected after 4 h.

(**I**) Assessment of IL-18 levels in cell supernatants following Δ*SPI-2* infection.

(**J–L**) Immunoblot analysis of caspase-1, IL-18 release, and cell images of BMDMs after *P. aeruginosa* (MOI, 1) infection for 4 h.

(**M–O**) Immunoblot analysis of caspase-1, IL-18 release, and cell images of BMDMs after *B. thailandensis* (MOI, 1) infection for 4 h.

Scale bars, 100 μm (C, L and O), NS, not significant; **P* < 0.05, ***P* < 0.01, ****P* < 0.001 and *****P* < 0.0001 (One-way ANOVA with Dunnett's multiple comparisons test). Data are

representative of 3 (**A, C, D, E, G, H, J, L, M, and O**) or from 3 (**B, F, I, K, and N**) independent experiments (mean ± SEM).

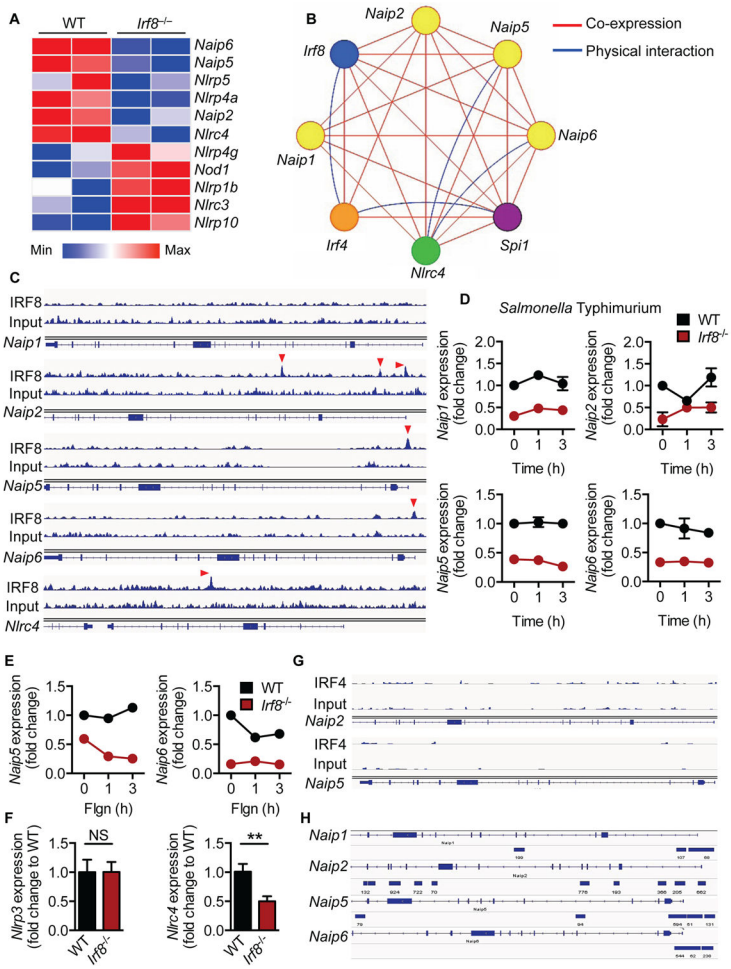

Figure 3. IRF8 is a key factor in transcriptional regulation of NAIPs

(**A**) Microarray analysis of the expression of pattern recognition receptor (PRR)–encoding genes 4 h after infection with *S.* Typhimurium (MOI, 0.1) in *Irf8*$^{-/-}$ BMDMs relative to that of WT.

(**B**) Interaction network visualizing the associations between IRF8, IRF4, SPI1, NLRC4, and NAIPs.

(**C**) Chromatin immunoprecipitation-sequencing (ChIP-seq) for IRF8 binding in *Naip1*, *Naip2*, *Naip5, Naip6,* and *Nlrc4*. Peaks indicate regions of DNA bound by IRF8.

(**D**) Real-time (RT)-PCR analysis of genes encoding NAIPs in BMDMs before (0 h) and after (1 h or 3 h) infection with *S.* Typhimurium, presented relative to levels of the gene encoding HPRT.

(**E**) RT-PCR analysis of genes encoding NAIP5 and NAIP6 in BMDMs before (0 h) and after (1 h or 3 h) transfection with 0.5 μg flagellin, presented relative to levels of the gene encoding HPRT.

(**F**) RT-PCR analysis of genes encoding NLRP3 and NLRC4 in untreated BMDMs, presented relative to levels of the gene encoding HPRT.

(**G**) ChIP-seq for IRF4 binding in *Naip2* and *Naip5*.

(**H**) ChIP-seq for SPI1 binding in *Naip1*, *Naip2*, *Naip5,* and *Naip6,* shown as MACS2 called peaks.

NS, not significant; and $^{**}P < 0.01$ (two-tailed *t* test). Data (**D–F**) are from 3 independent experiments (mean ± SEM).

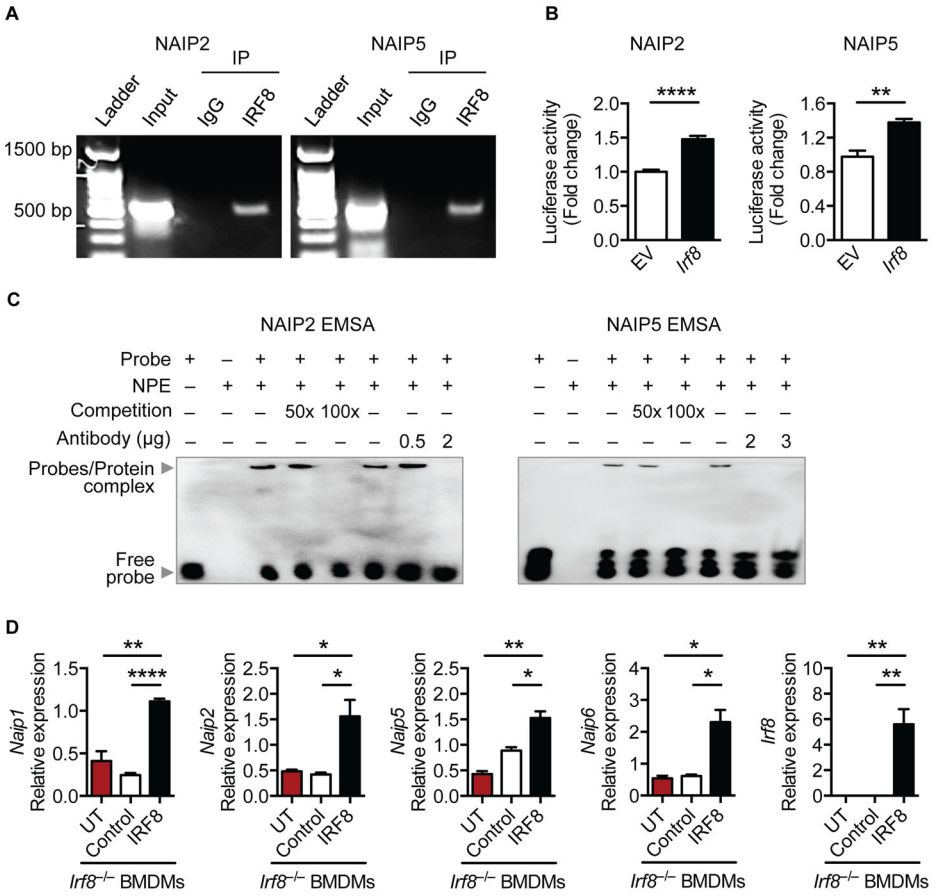

Figure 4. Transcriptional activity of IRF8 for *Naip*s

(**A**) ChIP for IRF8 followed by semi-quantitative PCR for *Naip2* or *Naip5* promoters were performed in BMDMs.

(**B**) Relative reporter luciferase activity for *Naip2* or *Naip5* promoters in IRF8 overexpressing cells, presented as fold change with respect to empty vector (EV) transfected cells. Data was normalized for transfection efficiency by normalizing firefly luciferase activity with renilla luciferase activity.

(**C**) Electrophoretic mobility shift assay was performed with *Naip2* or *Naip5* oligonucleotide probes incubated with nuclear protein extracts (NPE) from BMDMs.

(**D**) RT-PCR analysis of *Naip1*, *Naip2*, *Naip5*, *Naip6*, and *Irf8* in *Irf8*$^{-/-}$ BMDMs transfected with control or *Irf8* vectors, normalized to levels of *Gapdh*.

NS, not significant; *$P < 0.05$, **$P < 0.01$, ***$P < 0.001$ and ****$P < 0.0001$ (two-tailed t test). Data are representative of 2 (**A and C**) or from 2 (**B and D**) independent experiments (mean ± SEM).

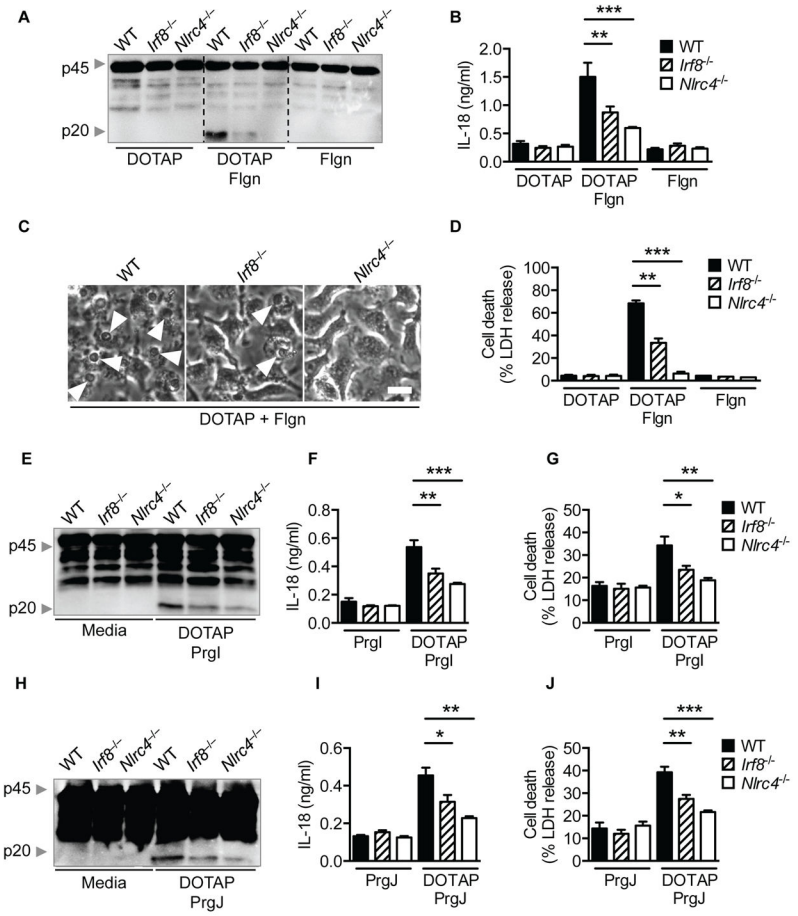

Figure 5. NLRC4 inflammasome activation in response to isolated bacterial proteins is impaired in the absence of IRF8

(**A–D**) BMDMs were treated with the liposomal agent DOTAP alone, transfected with 0.5 μg flagellin (DOTAP + Flgn), or treated with 0.5 μg flagellin (Flgn) alone.

(**A**) Immunoblot analysis of caspase-1.

(**B**) Assessment of IL-18 levels in cell supernatants.

(**C**) Microscopic analysis.

(**D**) Cell death was assessed by evaluating the release of lactate dehydrogenase (LDH).

(**E–G**) Immunoblot analysis of caspase-1, IL-18 release, and cell death in BMDMs transfected with PrgI (DOTAP + PrgI) or treated with PrgI alone.

(**H–I**) Immunoblot analysis of caspase-1, IL-18 release, and cell death in BMDMs transfected with PrgJ (DOTAP + PrgJ) or treated with PrgJ alone.

Scale bars, 100 μm (C), NS, not significant; *$P < 0.05$, **$P < 0.01$ and ***$P < 0.001$ (One-way ANOVA with Dunnett's multiple comparisons test). Data are representative of 3 (**A and C**) or 2(**E and H**) or from 3 (**B and D**) or 2 (**F, G, I, and J**) independent experiments (mean ± SEM).

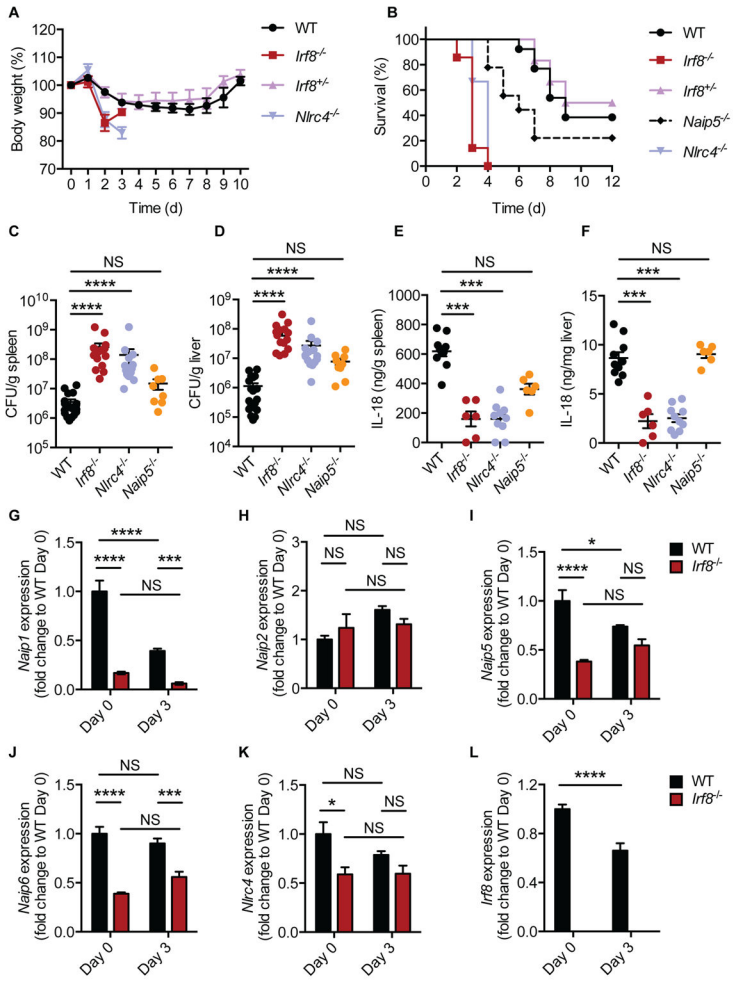

Figure 6. IRF8 confers protection against *S.* Typhimurium *in vivo*

(**A**) Body weight of 8-week-old WT (n=13), *Irf8*$^{-/-}$ (n=7), *Irf8*$^{+/-}$ (n=6) and *Nlrc4*$^{-/-}$ (n=9) mice infected intraperitoneally with 10^3 CFU of *S.* Typhimurium.

(**B**) Survival of WT (n=13), *Irf8*$^{-/-}$ (n=7), *Irf8*$^{+/-}$ (n=6), *Naip5*$^{-/-}$ (n=9) and *Nlrc4*$^{-/-}$ mice (n=9) infected as (**A**).

(**C and D**) Bacterial burden in the spleen and liver of WT (n=20), *Irf8*$^{-/-}$ (n=15), *Nlrc4*$^{-/-}$ (n=15) and *Naip5*$^{-/-}$(n=9) mice on day 3 after infection as (**A**).

(**E and F**) Analysis of IL-18 in the spleen and liver collected from WT (n=10), *Irf8*$^{-/-}$ (n=6), *Nlrc4*$^{-/-}$ (n=10) and *Naip5*$^{-/-}$ (n=6) mice on day 3 after infection as (**A**).

(**G–L**) RT-PCR analysis of genes encoding NAIPs, NLRC4, and IRF8 in the spleen collected from WT and *Irf8*$^{-/-}$ mice before infection (day 0) and after infection (day 3) as (**A**), presented relative to that of the gene encoding HPRT.

NS, not significant; **P* < 0.05, ****P* < 0.0001 and *****P* < 0.0001 (log-rank test [**B**], ANOVA with Dunn's multiple comparisons test [**C–F**], or Two-way ANOVA with Tukey's multiple comparisons test [**G–L**]). Data are from 2 experiments.

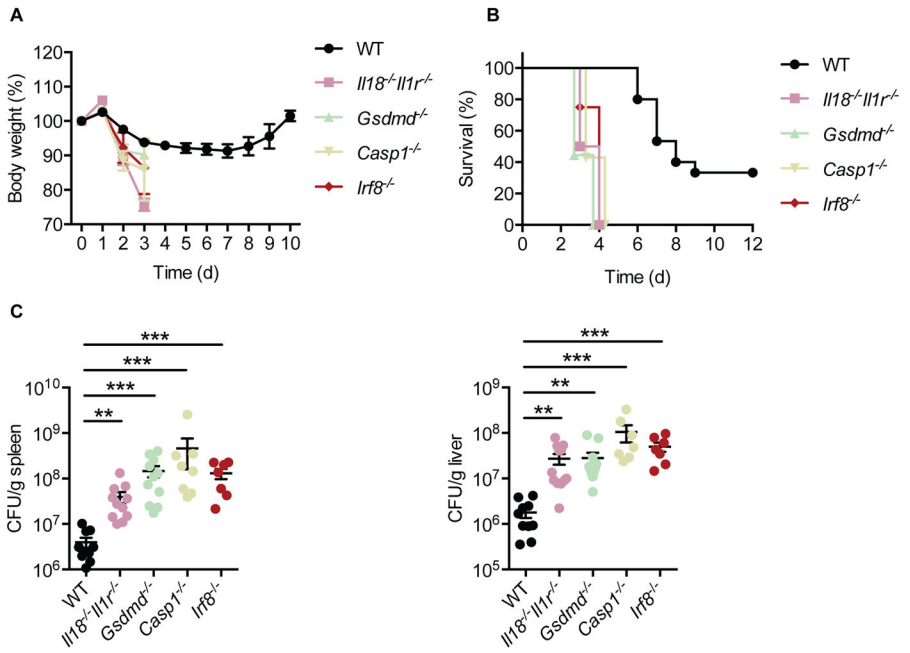

Figure 7. Inflammasome-dependent cytokines and pyroptosis both contribute to protection against *S.* Typhimurium infection *in vivo*

(**A**) Body weight of 8-week-old WT (n=13), *Il18*$^{-/-}$*Il1r*$^{-/-}$ (n=4), *Gsdmd*$^{-/-}$ (n=9), *Casp1*$^{-/-}$ (n=7), and *Irf8*$^{-/-}$ (n=8) mice infected intraperitoneally with 10^3 CFU of *S.* Typhimurium. (**B**) Survival of WT (n=13), *Il18*$^{-/-}$*Il1r*$^{-/-}$ (n=4), *Gsdmd*$^{-/-}$ (n=9), *Casp1*$^{-/-}$ (n=7), and *Irf8*$^{-/-}$ (n=8) mice infected as (**A**).

(**C**) Bacterial burden in tissues. For spleen, WT (n=10), *Il18*$^{-/-}$*Il1r*$^{-/-}$ (n=11), *Gsdmd*$^{-/-}$ (n=11), *Casp1*$^{-/-}$ (n=8), and *Irf8*$^{-/-}$ (n=7) mice; for liver, WT (n=10), *Il18*$^{-/-}$*Il1r*$^{-/-}$ (n=12), *Gsdmd*$^{-/-}$ (n=11), *Casp1*$^{-/-}$ (n=7), and *Irf8*$^{-/-}$ (n=7) mice on day 3 after infection as (**A**). NS, not significant; $^{**}P < 0.001$ and $^{***}P < 0.0001$ (log-rank test [**B**] or ANOVA with Dunn's multiple comparisons test [**C**]). Data are from 1 experiment.